Synthesis, Structure, and Reactivity of Three-Coordinate Vanadium(III) Chalcogenolates and Vanadium(V) Chalcogenide Chalcogenolates

Christopher P. Gerlach and John Arnold*

Department of Chemistry, University of California, Berkeley, California 94720-1460

Received April 24, 1996[⊗]

Reaction between $[(Me_3Si)_2N]_2V(Br)(THF)$ and $(THF)_2LiER$ (E = Se,Te; R = $Si(SiMe_3)_3$, $SiPh_3$) afforded the three-coordinate $[(Me_3Si)_2N]_2VER$ complexes in 60−80% yield. The $-SeSi(SiMe_3)_3$ complex and both of the −TeR derivatives were characterized crystallographically, and their X-ray structures are presented for comparative purposes. The structures feature a three-coordinate vanadium center with agostic interactions between two C−H groups of the amido trimethylsilyl ligands at the vacant apical coordination sites of vanadium. Reaction of $[(Me_3Si)_2N]_2V(Br)(THF)$ with $(DME)LiSeC(SiMe_3)_3$ (DME = 1,2-dimethoxyethane) afforded the vanadium(IV) dimer $\{[(Me_3Si)_2N]_2V(\mu\text{-Se})\}_2$ in moderate yield. X-ray crystallography confirmed a dimeric structure in the solid state with a long V−V distance of 3.044(1) Å. The three-coordinate compounds were oxidized by styrene oxide, propylene sulfide, and Ph_3PSe or Se to yield the oxo−, sulfide−, and selenide−vanadium(V) complexes, respectively; these derivatives were characterized by ^1H, $^{13}C\{^1H\}$, and ^{51}V NMR spectroscopy. $[(Me_3Si)_2N]_2V(E')[SeSi(SiMe_3)_3]$ (E′ = O, S, Se) and $[(Me_3Si)_2N]_2V(O)[TeSi(SiMe_3)_3]$ were isolated as deeply colored, crystalline solids and $[(Me_3Si)_2N]_2V(Se)[SeSi(SiMe_3)_3]$ was characterized crystallographically. Styrene oxide also reacted with $[(Me_3Si)_2N]_2V(Br)(THF)$ affording $[(Me_3Si)_2N]_2V(O)(Br)$ as orange crystals in 70% yield. In general, the vanadium(V) selenolates are more stable than the tellurolates, the latter being susceptible to reduction. For example, $[(Me_3Si)_2N]_2V(E)[TeSi(SiMe_3)_3]$ (E = S, Se) cleanly decomposes in solution affording $Te_2[Si(SiMe_3)_3]_2$ and $\{[(Me_3Si)_2N]_2V(\mu\text{-E})\}_2$. The compounds $[(Me_3Si)_2N]_2V(O)(X)$ (X = Br, $SeSi(SiMe_3)_3$) thermally rearrange to the siloxide−imido species, $[(Me_3Si)_2N](Me_3SiN)V(OSiMe_3)(X)$. The isomerization occurs more readily when X = Br, where kinetic data demonstrated the reaction to be first order in starting material, implicating an intramolecular 1,3-trimethylsilyl migration from N to O. Activation parameters ($\Delta H^{\ddagger} = 26 \pm 1$ kcal mol^{-1} and $\Delta S^{\ddagger} = -0.60 \pm 2$ eu) are in the range of those determined for the related thermal rearrangement of β-ketosilanes to siloxyalkenes.

Introduction

Although three-coordinate transition metal complexes are relatively rare compared to species with coordination numbers 4−6,[1] numerous studies have shown they undergo interesting reactivity toward a variety of substrates.[2,3] We have been studying the chemistry of selenolate and tellurolate complexes[4] of unsaturated early transition metals in order to probe structure and reactivity effects of coordination of a soft chalcogenolate ligand to an electrophilic metal.[5−10] Here we describe the synthesis, structure, and reactivity of a series of three-coordinate, bis(amido)vanadium(III) silyl selenolates and tellurolates. Only two other selenolate or tellurolate complexes of vanadium have appeared in the literature[11,12] both of which contain Cp (η^5-C_5H_5) or Cp* (η^5-C_5Me_5) ligands that tend to electronically and sterically saturate the metal center. We also describe oxidation reactions of the vanadium(III) chalcogenolates that lead to vanadium(V) chalcogenide chalcogenolates, and the crystal structure of a rare $[V{=}Se]^{3+}$ moiety is reported. Degradation of the vanadium(V) chalcogenides via isomerization or reduction of the metal center was also explored, and the results of these investigations are also presented.

Experimental Section

General Information. Standard inert atmosphere glovebox and Schlenk-line techniques were employed for all manipulations. All solvents were predried over 4 Å molecular sieves and, in the case of benzene, hexanes, and hexamethyldisiloxane (HMDSO), were distilled from sodium/benzophenone under N_2. Toluene was distilled from sodium. NMR solvents were dried similarly and were vacuum transferred prior to use. The compounds $(THF)_2LiESi(SiMe_3)_3$ (E = Se,[13] Te[14]), $(THF)_3LiTeSiPh_3$,[15] $(DME)LiSeC(SiMe_3)_3$,[13] and Ph_3PSe[16] were prepared by literature procedures; $(THF)_2LiSeSiPh_3$ was prepared analogously to the tellurolate. The synthesis of $[(Me_3Si)_2N]_2V(Br)(THF)$ was analogous to that for the chloride except that $VBr_3(THF)_3$ was substituted for the chloride.[17] Styrene oxide and propylene sulfide were purchased from commercial suppliers and distilled prior to use. Selenium powder was purchased from Aldrich and used as received.

* Author to whom correspondence should be addressed (email: arnold@violet.berkeley.edu).

⊗ Abstract published in *Advance ACS Abstracts,* September 1, 1996.

(1) Cotton, F. A.; Wilkinson, G. *Advanced Inorganic Chemistry,* 5th ed.; Wiley: New York, 1988.
(2) Eller, P. G.; Bradley, D. C.; Hursthouse, M. B.; Meek, D. W. *Coord. Chem. Rev.* **1977**, *24,* 1.
(3) For recent examples, see: Odom, A. L.; Cummins, C. C. *Organometallics* **1996**, *15*, 898. Laplaza, C. E.; Johnson, A. R.; Cummins, C. C. *J. Am. Chem. Soc.* **1996**, *118*, 709 and references therein.
(4) For a review on transition metal selenolates and tellurolates, see: Arnold, J. In *Progress in Inorganic Chemistry*; Karlin, K. D., Ed.; John Wiley & Sons: New York, 1995; Vol. 43, p 353.
(5) Christou, V.; Arnold, J. *J. Am. Chem. Soc.* **1992**, *114,* 6240.
(6) Christou, V.; Wuller, S. P.; Arnold, J. *J. Am. Chem. Soc.* **1993**, *115,* 10545.
(7) Christou, V.; Arnold, J. *Angew. Chem., Int. Ed. Engl.* **1993**, *32,* 1450.
(8) Cary, D. R.; Arnold, J. *J. Am. Chem. Soc.* **1993**, *115,* 2520.
(9) Cary, D. R.; Arnold, J. *Inorg. Chem.* **1994**, *33,* 1791.
(10) Cary, D. R.; Ball, G. E.; Arnold, J. *J. Am. Chem. Soc.* **1995**, *117,* 3492.
(11) Sato, M.; Yoshida, T. *J. Organomet. Chem.* **1975**, *87,* 217.
(12) Herberhold, M.; Schrepfermann; Rheingold, A. L. *J. Organomet. Chem.* **1990**, *394,* 113.
(13) Bonasia, P. J.; Christou, V.; Arnold, J. *J. Am. Chem. Soc.* **1993**, *115,* 6777.
(14) Bonasia, P. J.; Gindelberger, D. E.; Dabbousi, B. O.; Arnold, J. *J. Am. Chem. Soc.* **1992**, *114,* 5209.
(15) Gindelberger, D. E.; Arnold, J. *Organometallics* **1994**, *13,* 4462.
(16) Nicpon, P.; Meek, D. W. *Inorg. Chem.* **1966**, *5,* 1297.

S0020-1669(96)00439-9 CCC: $12.00

All NMR spectra were recorded in C_6D_6 at room temperature unless otherwise noted. Chemical shifts (δ) for ^{1}H and ^{13}C{^{1}H} NMR spectra are reported relative to tetramethylsilane and were calibrated relative to the chemical shift of the residual protium (^{1}H) or the ^{13}C{^{1}H} signal of the solvent. ^{51}V{^{1}H} NMR spectra were recorded at 78.94 MHz and externally referenced to neat $VOCl_3$ at 0 ppm. Samples for IR spectroscopy were prepared as Nujol mulls between KBr plates. Melting points were determined in sealed capillary tubes under nitrogen and are uncorrected. Samples for UV−vis spectroscopy were prepared in quartz cells under N_2 as dilute hexanes solutions (ca. 10^{-4}−10^{-5} M). Magnetic susceptibility measurements were made on solid samples with a Johnson-Mathey balance. Elemental analyses and electron impact mass spectrometry EI-MS measurements were done within the College of Chemistry, University of California, Berkeley. X-ray crystallography was performed at the University of California at Berkeley Chemistry X-ray Facility (CHEXRAY, Dr. F. J. Hollander, supervisor).

[(Me$_3$Si)$_2$N]$_2$VSeSi(SiMe$_3$)$_3$. Hexanes (50 mL) were added to a mixture of [(Me$_3$Si)$_2$N]$_2$V(Br)(THF) (2.14 g, 4.09 mmol) and (THF)$_2$LiSeSi(SiMe$_3$)$_3$ (1.95 g, 4.09 mmol). The forest green mixture was stirred for 30 min, and then the volatiles were removed under reduced pressure. The solid residue was extracted into HMDSO (45 mL) and the red-brown filtrate was concentrated to 10 mL and slowly cooled to −35 °C. The forest green product was isolated in two crops by filtration (2.31 g, 81%). Mp: 94−95 °C dec. IR: 1294 (w), 1248 (s), 979 (s), 956 (s), 849 (s, sh), 836 (vs), 782 (m), 755 (w), 687 (m), 669 (w), 637 (w), 622 (m), 625 cm^{-1} (sh). ^{1}H NMR (300 MHz): δ 1.00 (s, $\Delta\nu_{1/2}$ ca. 60 Hz). μ = 2.65 μ_B. UV−vis [λ, nm (ϵ)]: 216 (14 800); tails out to about 600 nm. Anal. Calcd for $C_{21}H_{63}N_2SeSi_8V$: C, 36.12; H, 9.09; N, 4.01. Found: C, 35.74; H, 9.12; N, 3.36.

[(Me$_3$Si)$_2$N]$_2$VTeSi(SiMe$_3$)$_3$. The procedure was analogous to that used for the selenolate; a reaction between [(Me$_3$Si)$_2$N]$_2$V(Br)(THF) (505 mg, 0.964 mmol) and (THF)$_2$LiTeSi(SiMe$_3$)$_3$ (508 mg, 0.965 mmol) yielded 481 mg (61%) of brown, crystalline product. Mp: 105−106 °C dec. IR: 1291 (w), 1245 (s), 1059 (m), 978 (s), 954 (s), 881 (sh), 843 (vs), 782 (s), 754 (w), 735 (w), 688 (m), 669 (m), 636 (w), 623 (m), 613 cm^{-1} (m). ^{1}H NMR (300 MHz): δ 0.84 (s, $\Delta\nu_{1/2}$ ca. 50 Hz). μ = 2.65 μ_B. UV−vis [λ, nm (ϵ)]: 220 (19 400); 236 sh (17 500); tails out to about 700 nm. Anal. Calcd for $C_{21}H_{63}N_2TeSi_8V$: C, 33.77; H, 8.50; N, 3.75. Found: C, 33.62; H, 8.72; N, 3.40.

[(Me$_3$Si)$_2$N]$_2$VSeSiPh$_3$. Toluene (30 mL) was added to a mixture of [(Me$_3$Si)$_2$N]$_2$V(Br)(THF) (2.01 g, 3.83 mmol) and (THF)$_2$LiSeSiPh$_3$ (1.87 g, 3.82 mmol). The green mixture was stirred for 4 h, and then the volatiles were removed under reduced pressure. The purple solid was extracted into toluene and filtered through a frit with Celite. The filtrate was concentrated and cooled to −35 °C. The product was isolated as dark purple crystals in two crops (1.83 g, 67%). Mp: 140−143 °C dec. IR: 1301 (w), 1248 (s), 1104 (s), 985 (s), 967 (s), 878 (m), 840 (s), 777 (m), 756 (w), 736 (m), 722 (m), 706 (m), 696 (m), 670 (m), 637 (w), 613 (w), 506 (m), 495 (m), 486 cm^{-1} (m). μ = 2.45 μ_B. Anal. Calcd for $C_{30}H_{51}N_2SeSi_5V$: C, 50.75; H, 7.24; N, 3.95. Found: C 50.76; H, 7.24; N, 3.83.

[(Me$_3$Si)$_2$N]$_2$VTeSiPh$_3$. The procedure was the same as for the analogous selenolate; a reaction between [(Me$_3$Si)$_2$N]$_2$V(Br)(THF) (1.79 g, 3.41 mmol) and (THF)$_3$LiTeSiPh$_3$ (2.08 g, 3.41 mmol) afforded 1.56 g (60%) of the product as brown crystals. Mp: 130−135 °C dec. IR: identical to the selenolate derivative. μ = 2.52 μ_B. Satisfactory elemental analyses were not obtained even for recrystallized material. Characterization rests upon the clean conversion to the diamagnetic [(Me$_3$Si)$_2$N]$_2$V(O)(TeSiPh$_3$), the IR spectrum (i.e., the same as for the −SeSiPh$_3$ derivative), and the crystallographic study.

{**[(Me$_3$Si)$_2$N]$_2$V(μ-Se)**}$_2$. **Method A.** [(Me$_3$Si)$_2$N]$_2$VTeSi(SiMe$_3$)$_3$ (991 mg, 1.33 mmol) and Se (105 mg, 1.33 mmol) were mixed with toluene (20 mL). The mixture was stirred for 2 days during which time it became increasingly green. The volatiles were removed under reduced pressure, and the brown solid was extracted with hexanes (40 mL). The emerald green filtrate was concentrated to ca. 15 mL and cooled to −35 °C for 24 h. A first crop of 230 mg of dark green needles was isolated by filtration. Concentration and cooling of the filtrate afforded a second crop of 302 mg (net yield 89%). The product obtained from the reaction consistently had an unknown impurity (^{1}H NMR (300 MHz): δ 1.15; one SiMe$_3$ group for the impurity per four SiMe$_3$ groups per product) whose quantity was significantly decreased on recrystallization from hexanes.

Method B. [(Me$_3$Si)$_2$N]$_2$V(Br)(THF) (1.55 g, 2.96 mmol) and (DME)LiSeC(SiMe$_3$)$_3$ (1.21 g, 2.96 mmol) were mixed with hexanes (30 mL) giving an emerald green solution. The mixture was stirred for 1.5 h and the volatiles were removed under reduced pressure. Extraction with hexanes (30 mL) followed by concentration and cooling of the filtrate afforded 349 mg (26% on V) of dark emerald green needles. The product obtained via this route is analytically pure. Mp: 193−203 °C dec. IR: 1265 (sh), 1248 (s), 877 (sh), 847 (s), 782 (s), 758 (sh), 709 (m), 700 (m), 667 (m), 615 cm^{-1} (w). ^{1}H NMR (300 MHz): δ 0.71 (s, $\Delta\nu_{1/2}$ ca. 3 Hz). ^{13}C{^{1}H} NMR (100 MHz): δ 11.58 (s, $\Delta\nu_{1/2}$ ca. 6 Hz). μ = 0.58 μ_B (0.41 μ_B per V). UV−vis [λ, nm(ϵ)]: 230 (37 100); 308 (20 000); 360 (17 900); 616 (4 140). Anal. Calcd for $C_{12}H_{36}N_2SeSi_4V$: C, 31.98; H, 8.05; N, 6.22. Found: C, 32.39; H, 8.40; N, 5.95.

[(Me$_3$Si)$_2$N]$_2$V(O)(Br). PhCH(O)CH$_2$ (0.35 mL, 3.0 mmol) was added to a hexanes solution (20 mL) of [(Me$_3$Si)$_2$N]$_2$V(Br)(THF) (1.59 g, 3.03 mmol). The green solution immediately changed to orange-red. The mixture was stirred for 15 min, and then the volatiles were removed under reduced pressure. Extraction with HMDSO (2 × 65 mL) followed by concentration and cooling of the filtrate (−35 °C) afforded 993 mg (70%) of orange crystals that were isolated by filtration. Mp: 100−103 °C dec. IR: 1402 (w), 1306 (w), 1264 (s, sh), 1249 (s), 1050 (w, sh), 1004 (s), $\nu_{V=O}$), 897 (s, br), 874 (sh), 848 (vs, br), 779 (m), 784 (m), 767 (w), 767 (w), 734 (w), 716 (s), 689 (sh), 677 (s), 642 (s), 620 cm^{-1} (m). ^{1}H NMR (400 MHz): δ 0.44 (s). ^{13}C{^{1}H} NMR (100 MHz): δ 5.27 (s). ^{51}V{^{1}H} NMR: δ −18 (s, $\Delta\nu_{1/2}$ ca. 370 Hz). UV−vis [λ, nm (ϵ)]: 218 (9 660); 262 (6 070); 372 (4 450). Anal. Calcd for $C_{12}H_{36}BrN_2OSi_4V$: C, 30.82; H, 7.76; N, 5.99. Found: C, 30.95; H, 7.84; N, 5.73.

[(Me$_3$Si)$_2$N]$_2$V(O)[SeSi(SiMe$_3$)$_3$]. PhCH(O)CH$_2$ (87 μL, 0.76 mmol) was added to a solution of [(Me$_3$Si)$_2$N]$_2$VSeSi(SiMe$_3$)$_3$ (530 mg, 0.759 mmol) in hexanes (20 mL). The mixture immediately became wine-red and the volatiles were removed under reduced pressure. The red solid was extracted into HMDSO (20 mL) and filtered and the filtrate concentrated to ca. 5 mL and cooled to −35 °C. The dark red product was collected by filtration in two crops yielding 281 mg (52%). Mp: 112−115 °C dec. IR: 1248 (s), 1012 (s, $\nu_{V=O}$), 879 (vs), 848 (vs), 779 (m), 785 (m), 762 (m), 728 (m), 705 (s), 688 (w), 672 (m), 645 (w), 624 cm^{-1} (m). ^{1}H NMR (300 MHz): δ 0.51 (s, 36H); 0.38 (s, 27H). ^{13}C{^{1}H} NMR (100 MHz): δ 5.59 (s, amido); 1.35 (s, selenolate). ^{51}V{^{1}H} NMR: δ 245 (s, $\Delta\nu_{1/2}$ ca. 275 Hz). UV−vis [λ, nm (ϵ)]: 214 (23 200); 250 (8 900); 366 (6 620); 512 (4 210). EI-MS: 714 (M$^+$). Anal. Calcd for $C_{21}H_{63}N_2OSeSi_8V$: C, 35.31; H, 8.89; N, 3.92. Found: C, 35.09; H, 9.10; N, 3.68.

[(Me$_3$Si)$_2$N]$_2$V(O)[TeSi(SiMe$_3$)$_3$]. The procedure was the same as for the analogous selenolate; a reaction between [(Me$_3$Si)$_2$N]$_2$VTeSi(SiMe$_3$)$_3$ (530 mg, 0.710 mmol) and PhCH(O)(CH$_2$) (81 μL, 0.71 mmol) yielded 253 mg (47%) of dark blue-black crystals of [(Me$_3$Si)$_2$N]$_2$V(O)[TeSi(SiMe$_3$)$_3$] that dissolve affording deep aqua colored solutions. Mp: 80−100 °C (slow dec to a black oil). IR: identical to the selenolate; 1012 cm^{-1} (s, $\nu_{V=O}$). ^{1}H NMR (300 MHz): δ 0.52 (s, 36H); 0.41 (s, 27H). ^{13}C{^{1}H} NMR (100 MHz): δ 5.59 (s, amido); 1.35 (s, tellurolate). ^{51}V{^{1}H} NMR: δ 504 (s, $\Delta\nu_{1/2}$ = 400 Hz). UV−vis [λ, nm (ϵ)]: 222 (19 300); 332 (5 250); 386 (4 130); 622 (2 060). Due to the compound's photosensitivity in solution, it was isolated along with ca. 10% of Te$_2$[Si(SiMe$_3$)$_3$]$_2$ (^{1}H NMR) and thus was not obtained analytically pure.

Generation of [(Me$_3$Si)$_2$N]$_2$V(O)(SeSiPh$_3$). PhCH(O)CH$_2$ (3.7 μL, 0.033 mmol) was added to a C_6D_6 solution (0.5 mL) of [(Me$_3$Si)$_2$N]$_2$VSeSiPh$_3$ (23 mg, 0.033 mmol) to give a dark orange solution. Analysis by NMR spectroscopy indicated the formation of styrene and the product. ^{1}H NMR (300 MHz): δ 7.91 (m, *o*-Ph, 6H); 0.38 (s, SiMe$_3$, 36H). The signal for the *m*- and *p*-Ph hydrogens could not be assigned unambiguously due to the overlapping resonances of the styrene. ^{51}V{^{1}H} NMR: δ 155 (s, $\Delta\nu_{1/2}$ ca. 430 Hz).

Generation of [(Me$_3$Si)$_2$N]$_2$V(O)(TeSiPh$_3$). On adding PhCH(O)CH$_2$ (2.9 μL, 0.025 mmol) to [(Me$_3$Si)$_2$N]$_2$VTeSiPh$_3$ (20 mg, 0.026

(17) Berno, P.; Minhas, R.; Hao, S.; Gambarotta, S. *Organometallics* **1994**, *13*, 1052.

mmol) in C_6D_6, an ink-purple solution was formed which was analyzed by NMR spectroscopy. ^{1}H NMR (300 MHz): δ 7.93 (m, *o*-Ph, 6H); 0.40 (s, $SiMe_3$, 36H). The signal for the *m*- and *p*-Ph hydrogens could not be assigned unambiguously due to the overlapping resonances of the styrene. ^{51}V{^{1}H} NMR: δ 387 (s, $\Delta\nu_{1/2}$ ca. 550 Hz).

$[(Me_3Si)_2N]_2V(S)[SeSi(SiMe_3)_3]$. The procedure was similar to that for $[(Me_3Si)_2N]_2V(O)[SeSi(SiMe_3)_3]$; a reaction between $[(Me_3Si)_2N]_2VSeSi(SiMe_3)_3$ (806 mg, 1.15 mmol) and MeCH(S)CH_2 (91 μL, 1.2 mmol) yielded 525 mg (62%) of maroon product. Mp: 118−121 °C dec. IR: 1306 (w), 1248 (s), 850 (vs), 783 (m), 722 (m), 701 (m), 672 (m), 645 (w), 624 (m), 568 cm^{-1} (m, $\nu_{V=S}$) cm^{-1}. ^{1}H NMR (300 MHz): δ 0.56 (s, 36H); 0.41 (s, 27H). ^{13}C{^{1}H} NMR (100 MHz): δ 6.44 (s, amido); 1.91 (s, selenolate). ^{51}V{^{1}H} NMR: δ 1102 (s, $\Delta\nu_{1/2}$ ca. 300 Hz). UV−vis [λ, nm (ϵ)]: 218 (17 600); 322 (7 830); 450 (2 880). Anal. Calcd for $C_{21}H_{63}N_2SSeSi_8V$: C, 34.53; H, 8.69; N, 3.84. Found: C, 34.31; H, 8.89; N, 3.64.

Generation of $[(Me_3Si)_2N]_2V(S)[TeSi(SiMe_3)_3]$. MeCH(S)$CH_2$ (2.6 μL, 0.033 mmol) was added to a C_6D_6 solution (0.5 mL) of $[(Me_3Si)_2N]_2VTeSi(SiMe_3)_3$ (25 mg, 0.033 mmol). The black mixture was analyzed by NMR spectroscopy. ^{1}H NMR (300 MHz): δ 0.57 (s, 36H); 0.43 (s, 27H). ^{51}V{^{1}H} NMR: δ 1410 (s, $\Delta\nu_{1/2}$ ca. 375 Hz). Over 1 day, the solution developed a persistent maroon color that contained $Te_2[Si(SiMe_3)_3]_2$ (δ 0.36) and a product giving rise to a singlet at δ 0.52 that we tentatively formulate as $\{[(Me_3Si)_2N]_2V(\mu\text{-}S)\}_2$. The half-life of $[(Me_3Si)_2N]_2V(S)[TeSi(SiMe_3)_3]$ under these conditions is ca. 10 h.

Generation of $[(Me_3Si)_2N]_2V(S)(SeSiPh_3)$. MeCH(S)$CH_2$ (2.7 μL, 0.034 mmol) was added to a C_6D_6 solution (0.5 mL) of $[(Me_3Si)_2N]_2VSeSiPh_3$ (25 mg, 0.035 mmol). The mixture immediately became dark orange-red. Analysis by NMR spectroscopy indicated the formation of propene along with the product. ^{1}H NMR (300 MHz): δ 7.95 (m, *o*-Ph, 6H); 7.17 (m, *m*/*p*-Ph, 9H); 0.47 (s, amido, 36H). ^{51}V{^{1}H} NMR: δ 1012 (s, $\Delta\nu_{1/2}$ ca. 450 Hz).

Generation of $[(Me_3Si)_2N]_2V(S)(TeSiPh_3)$. MeCH(S)$CH_2$ (2.3 μL, 0.029 mmol) was added to a C_6D_6 solution (0.5 mL) of $[(Me_3Si)_2N]_2VTeSiPh_3$ (22 mg, 0.029 mmol). The mixture immediately became dark brown-red. Analysis by NMR spectroscopy indicated the formation of propene and the product. ^{1}H NMR (300 MHz): δ 7.96 (m, *o*-Ph, 6H); 7.1 (m, *m*/*p*-Ph, 9H); 0.47 (s, amido, 36H). ^{51}V{^{1}H} NMR: δ 1287 (s, $\Delta\nu_{1/2}$ ca. 430 Hz).

$[(Me_3Si)_2N]_2V(Se)[SeSi(SiMe_3)_3]$. Toluene (20 mL) was added to $[(Me_3Si)_2N]_2VSeSi(SiMe_3)_3$ (602 mg, 0.862 mmol) and Se (69 mg, 0.87 mmol) and the mixture stirred for 48 h, gradually becoming maroon in color. The volatiles were removed under reduced pressure and the maroon solid extracted into HMDSO (40 mL). Concentration and cooling of the filtrate to −35 °C afforded the product as dark maroon needles in two crops (350 mg, 52%). Mp: 123−126 °C. IR: 1306 (w), 1262 (sh), 1246 (s), 1057 (w), 872 (sh), 846 (vs), 783 (m), 719 (m), 699 (m), 675 (m), 644 (w), 623 (m), 455 cm^{-1} (m, $\nu_{V=Se}$). ^{1}H NMR (300 MHz): δ 0.59 (s, 36H); 0.42 (s, 27H). ^{13}C{^{1}H} NMR (75 MHz): δ 6.71 (s, amido); 2.05 (s, selenolate). ^{51}V{^{1}H} NMR: δ 1444 (s, $\Delta\nu_{1/2}$ = 270 Hz). UV−vis [λ, nm (ϵ)]: 222 (17 000); 328 (5 510). Anal. Calcd for $C_{21}H_{63}N_2Se_2Si_8V$: C, 32.45; H, 8.17; N, 3.60. Found: C, 32.46; H, 8.29; N, 3.61.

Generation of $[(Me_3Si)_2N]_2V(Se)[TeSi(SiMe_3)_3]$. $[(Me_3Si)_2N]_2VTeSi(SiMe_3)_3$ (23 mg, 0.030 mmol) and Ph_3PSe (10 mg, 0.030 mmol) were mixed with C_6D_6 (0.5 mL) affording a dark maroon mixture. Analysis by ^{1}H and ^{51}V NMR spectroscopy indicated the formation of Ph_3P and $[(Me_3Si)_2N]_2V(Se)[TeSi(SiMe_3)_3]$. ^{1}H NMR (300 MHz): δ 0.61 (s, 36H); 0.44 (s, 27H). ^{51}V NMR: δ 1755 ($\Delta\nu_{1/2}$ ca. 410 Hz). After 6 h at room temperature under ambient lighting, the mixture was emerald green in color. Analysis by ^{1}H and ^{31}P{^{1}H} NMR spectroscopy showed only Ph_3P, $\{[(Me_3Si)_2N]_2V(\mu\text{-}Se)\}_2$ (δ 0.71 (s)), and $Te_2[Si(SiMe_3)_3]_2$ (δ 0.36 (s)).

Generation of $[(Me_3Si)_2N]_2V(Se)(SeSiPh_3)$. $[(Me_3Si)_2N]_2VSeSiPh_3$ (24 mg, 0.034 mmol) and Ph_3PSe (12 mg, 0.034 mmol) were mixed with C_6D_6 (0.5 mL) giving a dark orange-red mixture. Analysis by NMR spectroscopy indicated the formation of Ph_3P and the product. ^{1}H NMR (300 MHz): δ 7.96 (m, *o*-Ph, 6H); 0.51 (s, amido, 36H); the signal for the *m*/*p*-Ph hydrogens could not be unambiguously assigned due to the overlapping resonances of the Ph_3P. ^{51}V{^{1}H} NMR: δ 1369 ($\Delta\nu_{1/2}$ ca. 460 Hz).

Generation of $[(Me_3Si)_2N]_2V(Se)(TeSiPh_3)$. $[(Me_3Si)_2N]_2VTeSiPh_3$ (20 mg, 0.026 mmol) and Ph_3PSe (9 mg, 0.03 mmol) were mixed with C_6D_6 (0.5 mL) giving a dark orange-red mixture. Analysis by NMR spectroscopy indicated the formation of Ph_3P and the product. ^{1}H NMR (300 MHz): δ 7.96 (m, *o*-Ph, 6H); 0.51 (s, amido, 36H); the signal for the *m*/*p*-Ph hydrogens could not be unambiguously assigned due to the overlapping resonances of the Ph_3P. ^{51}V{^{1}H} NMR: δ 1648 ($\Delta\nu_{1/2}$ ca. 400 Hz).

$[(Me_3Si)_2N](Me_3SiN)V(OSiMe_3)(Br)$. $[(Me_3Si)_2N]_2V(O)(Br)$ (442 mg, 0.945 mmol) was dissolved in toluene (35 mL) and the solution heated at reflux for 1 h. The solvent was removed under reduced pressure giving a yellow-brown oil that was dried under vacuum. IR: 1250 (s), 1102 (s), 1018 (w), 945 (s), 892 (s), 868 (sh), 843 (s), 803 (s), 753 (m), 729 (m), 692 (sh), 678 (m), 635 (m), 620 (w), 479 cm^{-1} (m). ^{1}H NMR (300 MHz, C_7D_8): δ 0.46 (s, 18 H, amido); 0.28 (s, 9H, imido or siloxide); 0.23 (s, 9H, imido or siloxide). ^{13}C{^{1}H} NMR (100 MHz, C_7D_8): δ 4.57 (amido); 2.15 (imido or siloxide); 0.96 (imido or siloxide). ^{51}V{^{1}H} NMR: δ -216 ($\Delta\nu_{1/2}$ ca. 215 Hz). EI-MS (high resolution): calcd 466.972 850 amu; found 466.972 542 amu.

$[(Me_3Si)_2N](Me_3SiN)V(OSiMe_3)[SeSi(SiMe_3)_3]$. A toluene solution (20 mL) of $[(Me_3Si)_2N]_2V(O)[SeSi(SiMe_3)_3]$ (558 mg, 0.781 mmol) was heated at reflux for 16 h. The wine-red mixture gradually became dark red-orange. The volatiles were removed under reduced pressure, the residue was extracted into HMDSO (20 mL), and then the solution was filtered from a small amount of precipitate. The filtrate was concentrated to ca. 3 mL and cooled to −78 °C for 12 h. The rust product was isolated by filtration (268 mg, 48%). Mp: 90−93 °C. IR: 1248 (s), 1095 (s), 927 (s), 892 (m), 842 (s), 798 (m), 752 (m), 723 (m), 688 (m), 635 (w), 623 cm^{-1} (m). ^{1}H NMR (300 MHz): δ 0.52 (s, 18H, amido); 0.42 (s, 9H, imido or siloxide); 0.39 (s, 27H, selenolate); 0.27 (s, 9H, imido or siloxide). ^{13}C{^{1}H} NMR (100 MHz): δ 5.42 (s, amido); 2.89 (s, imido or siloxide); 1.79 (s, imido or siloxide); 1.39 (s, selenolate). ^{51}V{^{1}H} NMR: δ 8.73 ($\Delta\nu_{1/2}$ ca. 325 Hz). UV−vis [λ, nm (ϵ)]: 224 (18 800); 300 (9 150); 358 (5 850); 468 (2 460). EI-MS: 714 (M^+). Anal. Calcd for $C_{21}H_{63}N_2OSeSi_8V$: C, 35.31; H, 8.89; N, 3.92. Found: C, 35.00; H, 8.79; N, 3.57.

X-ray Crystallography. A summary of crystal data, data collection, and refinement for all crystallographically characterized compounds is given in Table 1. Selected positional parameters are listed in Table 2.

$[(Me_3Si)_2N]_2VSeSi(SiMe_3)_3$. Crystals were grown by slowly cooling a saturated HMDSO solution of the compound to −35 °C. A crystal was mounted on a glass capillary with Paratone-N oil, transferred to a CAD4-diffractometer, and centered in a steam of cold dinitrogen gas. Cell constants and orientation matrix were obtained from the least-squares refinement of 24 carefully centered high-angle reflections. A 3.76% decrease in the intensities of three standard reflections (measured every 200 reflections) was observed during the experiment, and a linear decay correction was applied to the data. The data were corrected for Lorentz and polarization effects. An empirical absorption correction based on azimuthal scans near χ = 90° was applied to the data. For the overall averaged transmission curve, the transmission factors ranged 0.9622−0.9985. Inspection of the data and the intensity statistics indicated the centric space group $P\bar{1}$. The structure was solved by direct methods using the TEXSAN package[18] on a Digital VAX station and refined using standard least-squares and Fourier techniques. All of the non-hydrogen atoms were refined with anisotropic thermal parameters. The six hydrogen atoms (H(1)−H(3); H(19)−H(21)) of the agostic methyl groups (C(1) and C(7)) were located from a difference Fourier map and refined with isotropic thermal parameters. The remainder of the hydrogen atoms were introduced at idealized positions, then refined isotropically. Neutral atomic scattering factors were taken from Cromer and Waber,[19] and anomalous dispersion effects were included in F_c.[20] The final residuals for 550 variables refined against 4363 data for which $I > 3\sigma(I)$ were R = 0.0303, R_w = 0.0355, and GOF = 1.80.

(18) *TEXSAN: Crystal Structure Analysis Package*; Molecular Structure Corporation: 1992.

(19) Cromer, D. T.; Waber, J. T. *International Tables for X-ray Crystallography*; The Kynoch Press: Birmingham, England, 1974; Vol. IV, Table 2.2B.

Table 1. Summary of X-ray Diffraction Data: [N] = $N(SiMe_3)_2$; R = $Si(SiMe_3)_3$

	$[N]_2VSeR$	$[N]_2VTeR$	$[N]_2VTeSiPh_3$	$[N]_2V(Se)(SeR)$	$\{[N]_2V(\mu\text{-Se})\}_2$
formula	$C_{21}H_{63}N_2SeSi_8V$	$C_{21}H_{63}N_2Si_8TeV$	$C_{30}H_{51}N_2Si_5TeV$	$C_{21}H_{63}N_2Se_2Si_8V$	$C_{24}H_{72}N_4Se_2Si_8V_2$
MW	698.33	746.97	758.72	777.29	901.35
space group	$P\bar{1}$	$P\bar{1}$	$Pca2_1$	$p2_1/a$	$P2_1/c$
a (Å)	9.7976(39)	10.1913(2)	11.4250(2)	12.9318(3)	9.0555(4)
b (Å)	12.3166(37)	12.8922(3)	16.1541(3)	17.6877(4)	14.5256(7)
c (Å)	18.7887(50)	17.5831(4)	20.6208(1)	18.1551(4)	35.0622(15)
α (deg)	105.085(23)	93.202(1)	90	90	90
β (deg)	102.408(27)	103.143(1)	90	94.296(1)	95.087(1)
γ(deg)	105.241(27)	111.649(1)	90	90	90
vol (Å^3)	2010.127(1.482)	2065.92(12)	3805.76(11)	4141.01(25)	4588.31(60)
Z	2	2	4	4	4
d_{calcd} (g cm^{-3})	1.15	1.20	1.32	1.25	1.30
crystal size (mm)	0.50 × 0.50 × 0.10	0.31 × 0.22 × 0.20	0.24 × 0.09 × 0.07	0.23 × 0.34 × 0.15	0.40 × 0.10 × 0.12
radiation (λ/Å)	Mo Kα (0.7103)	Mo Kα (0.7103)	Mo Kα (0.7103)	Mo Kα (0.7103)	Mo Kα (0.7103)
scan mode	$\theta-2\theta$	Σ (0.3 deg scans)	Σ (0.3 deg scans)	Σ (0.3 deg scans)	Σ (0.3 deg scans)
2θ range (deg)	3−45	3−46.5	2−46.5	3−46.5	3−46.5
collcn range	$+h,\pm k,\pm l$	hemisphere	hemisphere	hemisphere	hemisphere
μ (cm^{-1})	14.02	11.77	11.90	22.43	22.23
total no reflcns	5712	8247	15471	12901	18578
no of unique reflcns	5257	5705	3103	6020	6855
reflcns with $I > 3\sigma(I)$	4363	4704	2690	4677	5055
R_{int}	0.031	0.046	0.125	0.038	0.065
final R,[a] R_w[b]	0.0303, 0.0355	0.0406, 0.0492	0.0519, 0.0475	0.0410, 0.0551	0.0446, 0.0550
GOF	1.80	2.00	1.45	2.23	1.91
T (°C)	−95	−84	−124	−100	−108

[a] $R = [\sum||F_o| - |F_c||]/\sum|F_o|$. [b] $R_w = \{[\sum w(|F_o| - |F_c|)^2]/\sum wF_o^2\}^{1/2}$.

$[(Me_3Si)_2N]_2VTeSi(SiMe_3)_3$. Crystals were grown from a concentrated HMDSO solution at −35 °C. A crystal was mounted on a glass capillary with Paratone-N oil, transferred to a Siemens SMART diffractometer/CCD area detector,[21] and centered in a steam of cold dinitrogen gas. A preliminary orientation matrix and unit cell parameters were determined by collecting 60 10-s frames, followed by spot integration and least-squares refinement. A hemisphere of data was collected using 0.3° ω scans at 30 s per frame. The raw data were integrated (*XY* spot spread = 1.60°; *Z* spot spread = 0.60°) and the unit cell parameters refined (5397 reflections with $I > 100(I)$) using SAINT.[22] Preliminary data analysis and an absorption correction (T_{min} = 0.683; T_{max}= 0.862) were performed using XPREP.[23] Of the 8247 reflections measured, 5705 were independent and the redundant reflections were averaged with a 4.6% internal consistency. No correction for crystal decay was applied to the data. Inspection of the data and the intensity statistics indicated the centric space group $P\bar{1}$. The structure was solved by direct methods using the TEXSAN package on a Digital microvax station and refined using standard least-squares and Fourier techniques. All non-hydrogen atoms were refined with anisotropic thermal parameters. The six hydrogen atoms (H(1)−H(3); H(19)−H(21)) of the agostic methyl groups (C(1) and C(7)) were located from a difference Fourier map and refined with isotropic thermal parameters. The remainder of the hydrogen atoms were introduced at idealized positions and used in the structure factor calculations but not refined. Neutral atomic scattering factors were taken from Cromer and Waber, and anomalous dispersion effects were included in F_c. The final residuals for 323 variables refined against 4704 data for which $I > 3\sigma(I)$ were R = 0.0406, R_w = 0.0492, and GOF = 2.00.

$[(Me_3Si)_2N]_2VTeSiPh_3$. Brown crystals were grown from toluene at −35 °C. Data collection and preliminary data analysis were conducted with a Siemens SMART diffractometer/CCD area detector and the programs SAINT and XPREP as described above. No correction for crystal decay was applied. The systematically absent data were consistent with either $Pca2_1$ or *Pbcm* as the space group; the intensity statistics implicated the acentric space group, and the structure was successfully solved and refined in $Pca2_1$ as described above. The lack of a mirror plane within the molecule (Z = 4) confirmed this choice. Refinement of the Flack parameter to near zero implicated the crystal as a single enantiomorph. Refinement carried out on the inverted structure gave values of R/R_w that were significantly higher. All non-hydrogen atoms were refined anisotropically except for C(1) and C(15), which were refined with isotropic thermal parameters. Hydrogen atoms were introduced at fixed, idealized positions and were included in the structure factor calculations but not refined. The final residuals for 342 variables refined against 2690 data for which $I > 3\sigma(I)$ were R = 0.0519, R_w = 0.0475, and GOF = 1.45.

$[(Me_3Si)_2N]_2V(Se)[SeSi(SiMe_3)_3]$. Deep burgundy crystals were grown from a concentrated HMDSO solution at −35 °C. Data collection and preliminary data analysis were conducted with a Siemens SMART diffractometer/CCD area detector and the programs SAINT and XPREP as described above. No correction for crystal decay was applied. The space group $P2_1/a$ was uniquely defined by the systematic absences. No correction for crystal decay was applied to the data. The structure was solved and refined as described above. All non-hydrogen atoms were refined with anisotropic thermal parameters; hydrogen atoms were introduced at fixed idealized positions and included in F_c but not refined. The final residuals for 307 variables refined against 4677 data for which $I > 3\sigma(I)$ were R = 0.0410, R_w = 0.0551, and GOF = 2.23.

$\{[(Me_3Si)_2N]_2V(\mu\text{-Se})\}_2$. Emerald green needles of the compound were grown from hexanes at −35 °C. Data collection and preliminary data analysis were conducted with a Siemens SMART diffractometer/CCD area detector and the programs SAINT and XPREP as described above. No correction for crystal decay was applied. The systematically absent data uniquely defined the space group $P2_1/c$. The structure was solved and refined as described above. All non-hydrogen atoms were refined with anisotropic thermal parameters; all hydrogen atoms were introduced at idealized, fixed positions and included in F_c but not refined. The final residuals for 361 variables refined against 5055 data for which $I > 3\sigma(I)$ were R = 0.0446, R_w = 0.0550, and GOF = 1.90.

Results and Discussion

Vanadium(III) Chalcogenolates. Salt metathesis reactions between $[(Me_3Si)_2N]_2V(Br)(THF)$ and 1 equiv of either $(THF)_2LiESi(SiMe_3)_3$ (E = Se, Te) or $(THF)_xLiESiPh_3$ (E = Se, Te) afforded the three-coordinate bis(bistrimethylsilylamido)

(20) Cromer, D. T.; Waber, J. T. *International Tables for X-ray Crystallography*; The Kynoch Press: Birmingham, England, 1974; Vol IV, Table 2.3.1.
(21) *SMART Area-Detector Software Package*; Siemens Industrial Automation, Inc.: Madison, WI, 1993.
(22) *SAINT: SAX Area-Detector Integration Program*, v. 4.024; Siemens Industrial Automation, Inc.: Madison, WI, 1994.
(23) *XPREP: Part of the SHELXTL Crystal Structure Determination Package*; Siemens Industrial Automation: Madison, WI, 1994.

Table 2. Atomic Coordinates for Selected Atoms of $[(Me_3Si)_2N]_2VSeSi(SiMe_3)_3$, $[(Me_3Si)_2N]_2VTeSi(SiMe_3)_3$, $[(Me_3Si)_2N]_2VTeSiPh_3$, $\{[(Me_3Si)_2N]_2V(\mu\text{-Se})\}_2$, and $[(Me_3Si)_2N]_2V(Se)[SeSi(SiMe_3)_3]$

atom	*x*	*y*	*z*	B_{eq} (Å)
		$[(Me_3Si)_2N]_2VSeSi(SiMe_3)_3$		
V	0.32052(6)	−0.05982(5)	0.77724(3)	1.91(2)
Se	0.55684(4)	0.09867(3)	0.80558(2)	2.58(1)
N(1)	0.2416(3)	−0.0803(2)	0.8599(2)	2.41(9)
N(2)	0.2306(3)	−0.1804(2)	0.6759(1)	2.34(9)
Si(1)	0.1325(1)	0.0087(1)	0.85856(6)	2.86(3)
Si(2)	0.2431(1)	−0.1760(1)	0.91333(6)	3.43(4)
Si(3)	0.3598(1)	−0.25210(9)	0.67451(6)	3.02(3)
Si(4)	0.0621(1)	−0.23219(9)	0.60374(6)	3.04(3)
Si(5)	0.5820(1)	0.25561(8)	0.75868(5)	1.98(3)
Si(6)	0.4045(1)	0.2209(1)	0.64123(6)	2.74(3)
Si(7)	0.6052(1)	0.43006(9)	0.85629(6)	2.90(3)
Si(8)	0.8115(1)	0.26815(9)	0.73598(6)	2.55(3)
		$[(Me_3Si)_2N]_2VTeSi(SiMe_3)_3$		
V	0.57730(9)	0.63571(7)	0.81214(5)	3.05(3)
Te	0.33254(4)	0.45319(3)	0.79907(2)	3.85(1)
N(1)	0.7654(4)	0.6270(3)	0.8427(2)	3.2(1)
N(2)	0.5624(5)	0.7803(3)	0.8043(2)	3.8(1)
Si(1)	0.7733(2)	0.6008(1)	0.93902(8)	3.80(5)
Si(2)	0.9155(2)	0.6598(1)	0.8040(1)	4.13(5)
Si(3)	0.5071(2)	0.7714(1)	0.7040(1)	4.30(6)
Si(4)	0.5918(2)	0.8895(1)	0.8761(1)	4.60(6)
Si(5)	0.2541(2)	0.2982(1)	0.68357(8)	3.36(5)
Si(6)	0.0790(2)	0.3147(1)	0.5776(1)	4.62(6)
Si(7)	0.4484(2)	0.2741(1)	0.64377(9)	4.03(5)
Si(8)	0.1383(2)	0.1437(1)	0.7434(1)	4.92(6)
		$[(Me_3Si)_2N]_2VTeSiPh_3$		
V	0.5006(2)	0.2068(1)	0.3593(1)	2.4(1)
Te	0.48675(7)	0.33118(4)	0.4009	2.84(4)
N(1)	0.6147(8)	0.1595(5)	0.4210(6)	2.4(6)
N(2)	0.3867(8)	0.1645(5)	0.2908(6)	2.3(5)
Si(1)	0.7400(3)	0.1783(2)	0.3655(3)	2.7(2)
Si(2)	0.6034(4)	0.1163(2)	0.5122(3)	3.0(2)
Si(3)	0.2605(4)	0.1645(2)	0.3489(3)	3.0(2)
Si(4)	0.4066(4)	0.1244(2)	0.1963(3)	3.1(2)
Si(5)	0.5297(3)	0.4065(2)	0.2829(3)	2.6(2)
		$\{[(Me_3Si)_2N]_2V(\mu\text{-Se})\}_2$		
Se(1)	0.55320(6)	0.30201(4)	0.35686(2)	3.27(3)
Se(2)	0.93781(6)	0.24399(4)	0.38305(2)	3.26(3)
V(1)	0.69781(9)	0.20333(6)	0.39921(2)	2.83(4)
V(2)	0.7933(1)	0.35254(6)	0.34589(2)	2.93(4)
Si(1)	0.7674(2)	−0.0109(1)	0.37261(4)	3.57(7)
Si(2)	0.4581(2)	0.0553(1)	0.38077(4)	3.54(7)
Si(3)	0.5749(2)	0.3123(1)	0.47251(5)	4.32(8)
Si(4)	0.7882(2)	0.1542(1)	0.48392(4)	3.37(7)
Si(5)	0.7018(2)	0.5572(1)	0.33811(6)	5.2(1)
Si(6)	0.9297(2)	0.5156(1)	0.40438(5)	4.37(8)
Si(7)	0.7083(2)	0.2660(1)	0.26146(5)	3.93(8)
Si(8)	1.0101(2)	0.3505(1)	0.28400(5)	4.38(8)
N(1)	0.6514(4)	0.0805(3)	0.3851(1)	2.8(2)
N(2)	0.6859(4)	0.2291(3)	0.4516(1)	3.2(2)
N(3)	0.8168(5)	0.4747(3)	0.3632(1)	3.5(2)
N(4)	0.8259(4)	0.3301(3)	0.2949(1)	3.2(2)
		$[(Me_3Si)_2N]_2V(Se)[SeSi(SiMe_3)_3]$		
Se(1)	0.83629(4)	0.14444(3)	0.24972(3)	4.50(3)
Se(2)	0.75306(3)	−0.05452(3)	0.24505(3)	3.20(2)
V	0.70616(6)	0.07137(4)	0.27028(4)	2.88(3)
Si(1)	0.6131(1)	0.14348(9)	0.1179(1)	5.01(8)
Si(2)	0.4791(1)	0.04248(8)	0.20921(9)	3.91(6)
Si(3)	0.6357(1)	0.1736(1)	0.3974(1)	5.21(8)
Si(4)	0.7280(1)	0.0206(1)	0.43853(9)	5.07(8)
Si(5)	0.9156(1)	−0.09896(7)	0.21903(7)	2.94(5)
Si(6)	0.9566(1)	−0.19820(8)	0.3024(1)	4.33(7)
Si(7)	1.0564(1)	−0.01473(7)	0.21735(9)	3.84(6)
Si(8)	0.8800(1)	−0.15355(9)	0.10086(9)	4.26(7)
N(1)	0.5962(3)	0.0928(2)	0.2015(2)	3.1(2)
N(2)	0.6767(3)	0.0837(2)	0.3695(2)	3.6(2)

vanadium(III) chalcogenolates in moderate to good yields (eq 1). While the trimethylsilyl derivatives are highly soluble in hexanes and are best crystallized from hexamethyldisiloxane (HMDSO), the triphenylsilyl complexes are insoluble in aliphatic hydrocarbon solvents, but readily crystallized from toluene.

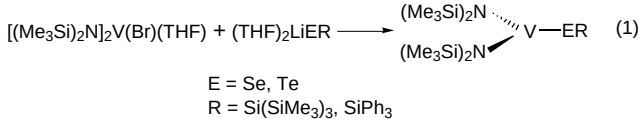

All of the compounds are paramagnetic with solid state magnetic moments (2.45−2.65 μ_{BM}) that are slightly lower than the spin-only prediction. Proton NMR spectra were generally featureless except in the case of the trimethylsilyl derivatives, where a single broad resonance was observed around 1 ppm. Similarly, the UV−vis spectra consisted of a single, broad absorbance at 216 nm (ϵ = 15 000 M^{-1} cm^{-1}) (E = Se) and 220 nm (19 000 M^{-1} cm^{-1}) (E = Te); these peaks both tailed out well into the visible region of the spectra, possibly obscuring any other lower intensity charge-transfer or d−d transitions. Significantly, there was no evidence for the presence of coordinated THF in the products. The lability of the THF during the course of the reaction is presumably due, at least in part, to the high steric demands of both the bulky amido ligands and the silyl chalcogenolates.

The X-ray structures of $[(Me_3Si)_2N]_2VESi(SiMe_3)_3$ (E = Se, Te) were determined for comparative purposes. While the geometrical parameters are similar, the structures are not isomorphous due to differences in crystal packing. An ORTEP view of the selenolate is shown in Figure 1 and selected bond distances and angles are in Table 3.

The coordination geometry about vanadium is trigonal planar (N(1)−V−N(2) = 119.2(1)°; Se−V−N(1) = 119.84(9)°; Se−V−N(2) = 120.15(9)°) with the mean deviation from the VN_2Se plane less than 0.07 Å. The V−Se single bond length (2.451(1) Å) appears normal in comparison to those in the ferrocenyl bisselenolate $(C_5H_4Se)_2FeV(O)(Cp^*)$ (V−Se = 2.393(2), 2.405(2) Å)[12] although at this point a more apt comparison in terms of coordination number and oxidation state of the vanadium is not available. The V−Se−Si angle (124.07(4)°) is in the middle of the range observed for structures of $-SeSi(SiMe_3)_3$ complexes. As expected, the geometry about the amido nitrogen atoms is also planar with the sum of the angles about N(1) and N(2) being 359.2(3)° and 359.5(3)°, respectively. The V−N and N−Si bond lengths are unexceptional ($V-N_{avg}$ = 1.926(4) Å; $N-Si_{avg}$ = 1.729(6) Å). In C_{2v} symmetry, π-bonding between the amido nitrogens and the vanadium is maximized when the angles between the amido planes and the trigonal plane are 0°; in actuality, steric repulsions between the bulky $-SiMe_3$ groups prevent this orientation. Nevertheless, in the present case the dihedral angles are larger than would be expected based on steric arguments alone (85° and 66° for the N(1) and N(2) amido groups, respectively) as a result of close, nonbonding contacts between two methyl groups of the $-N(SiMe_3)_2$ ligands and the vandium (V−C(1) = 2.504(4) Å; V−C(7) = 2.624(4) Å). The methyl hydrogen atoms were located and refined with each methyl group positioning a hydrogen atom in close proximity to the metal center (V−H(1) = 2.07(3) Å; V−H(19) = 2.17(3) Å). The agostic[24] methyl groups are oriented nearly at the apices of a trigonal pyramid about vanadium (C(1)−V−C(7) = 177.5(1)°; H(1)−V−H(19) = 172(1)°), and the dihedral angle between the C(1)VC(7) and the VN_2Se planes is 83°. The Si(1)−C(1) bond (1.894(4) Å) is elongated slightly compared to the Si(1)−C(2) and Si−C(3)

(24) Brookhart, M.; Green, M. L. H.; Wong, L.-L. *Prog. Inorg. Chem.* **1988**, *36*, 1.

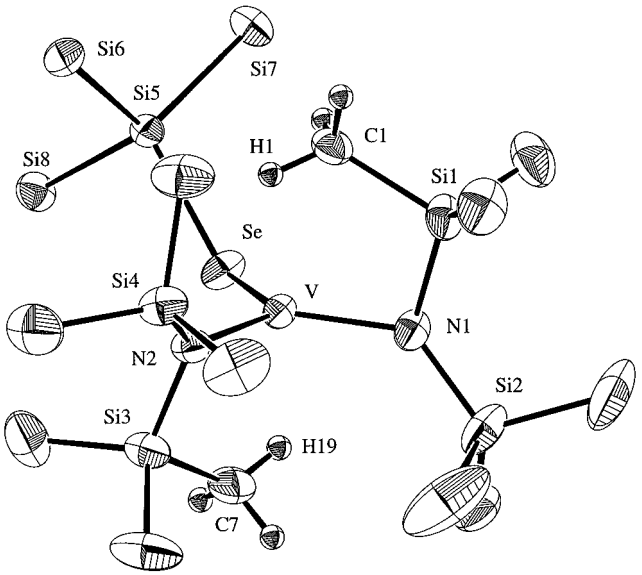

Figure 1. ORTEP drawing of $[(Me_3Si)_2N]_2VSeSi(SiMe_3)_3$. Thermal ellipsoids are drawn at 50% probability level. Methyl groups on $-SeSi(SiMe_3)_3$ have been omitted for clarity.

bond distances (1.855(5) and 1.866(4) Å, respectively). A similar effect is observed between the Si−C(7) and Si−C(8)/Si−C(9) bond lengths. The $-Si(SiMe_3)_3$ substituent on Se is displaced toward one of the amido ligands (Si(5)−Se−V−N(1) = 117.6(1)°; Si(5)−Se−V−N(2) = 72.9(1)°) such that it is directed away from the approach of an amido−$SiMe_3$ on the same side of the VN_2Se plane.

An ORTEP view of $[(Me_3Si)_2N]_2VTeSi(SiMe_3)_3$ is shown in Figure 2. As seen from the metrical parameters collected in Table 3, except for the bond lengths to tellurium, the structure is very similar to the silylselenolate. The V−Te bond distance (2.6758(9) Å) is about 0.2 Å longer than the V−Se bond length above, consistent with the difference between the covalent radii of the two chalcogens.[25] As is typical for the crystal structures of analogous $-Si(SiMe_3)_3$ complexes (E = Se or Te), the V−Te−Si angle of 117.70(4)° is smaller than that in the selenolate, an effect we attribute to (i) the larger size of the tellurium atom positioning the bulk of the $-Si(SiMe_3)_3$ fragment further away from the other ligands and (ii) the increased p-character in the Te-element bonds. An agostic interaction between two pendant methyl groups from the amido ligands and the vanadium is also evident in the tellurolate (V−C(1) = 2.613(6) Å; V−C(7) = 2.548(7) Å; V−H(1) = 2.16(6) Å; V−H(19) = 2.04(7) Å; C(1)−V−C(7) = 175.9(2)°; H(1)−V−H(19) = 168(3)°). The bulky silyl substituent on the tellurium is folded toward the N(1) amido substituent (N1-V-Te-Si5 = 71.8(1)°) in order to accommodate the axial approach of C(19) on the same side of the vanadium trigonal plane.

An ORTEP view of the structure of $[(Me_3Si)_2N]_2VTeSiPh_3$, which confirms the three-coordinate nature of the $-ESiPh_3$ derivatives, is shown in Figure 3. The metrical parameters about the vanadium and amido groups are similar to those in the above derivatives (Table 3). The V−Te (2.657(2) Å) and Te−Si (2.507(4) Å) distances are slightly shorter than those in the $-TeSi(SiMe_3)_3$ derivative and the V−Te−Si angle (113.3(1)°) is about 4° smaller. Related geometric differences were observed on comparing the X-ray structures of $Cp_2Zr[TeSi(SiMe_3)_3]_2$[6] and $Cp_2Zr(TeSiPh_3)_2$.[15] Two methyl groups of the $-N(SiMe_3)_2$ ligand are again in close contact with the vanadium (V−C(1) = 2.58(1) Å; V−C(7) = 2.70(1) Å; C(1)−V−C(7) = 177.1(5)°). It seems that the metal may be sufficiently electrophilic in $[(Me_3Si)_2N]_2VX$ type compounds, where X donates predominantly in a σ-manner to the metal, as to make these types of agostic interactions a general structural feature.

Interestingly, reaction of $[(Me_3Si)_2N]_2V(Br)(THF)$ with 1 equiv of (DME)LiSeC$(SiMe_3)_3$ (DME = 1,2-dimethoxyethane) did not give the expected $[(Me_3Si)_2N]_2VSeC(SiMe_3)_3$, but rather the bis($\mu$-Se)-bridged dimer $\{(Me_3Si)_2N]_2V(\mu\text{-Se})\}_2$, isolated in yields of about 30% (eq 2).

$$[(Me_3Si)_2N]_2V(Br)(THF) + (DME)LiSeC(SiMe_3)_3 \rightarrow \{[(Me_3Si)_2N]_2V(\mu\text{-Se})\}_2 + HC(SiMe_3)_3 + ... \quad (2)$$

The reaction proceeded immediately in hexanes at room temperature with the primary organic material, after crystallization of the product, being $HC(SiMe_3)_3$ (^{1}H NMR). The vanadium(IV)−vanadium(IV) dimer is weakly paramagnetic in the solid state (μ = 0.58 μ_B). Sharp, nonshifted singlets are observed in the ^{1}H and $^{13}C\{^1H\}$ NMR spectra; however, no ^{77}Se or ^{51}V NMR signals were detected. In contrast to the rather featureless electronic spectra of the three-coordinate vanadium(III) derivatives, that of the dimer shows several charge-transfer absorptions at 230 nm (37 100 M^{-1} cm^{-1}), 308 nm (20 000 M^{-1} cm^{-1}), 360 nm (18 000 M^{-1} cm^{-1}), and 616 nm (4 000 M^{-1} cm^{-1}), the latter responsible for the intense green color of the compound in solution.

The mechanism of the formation of $\{[(Me_3Si)_2N]_2V(\mu\text{-Se})\}_2$, particularly the details of the Se−C bond scission, remains unclear. While S−C bond cleavage in thiolates is relatively common,[26] for the most part these reactions involve nucleophilic attack on the thiolate carbon atom. Given the weakness of C−Se bonds,[27] we favor a mechanism involving homolysis of this bond followed by dimerization to form the vanadium selenide product. We also note that the dearylation of phenylselenolate to produce $[PPh_4]_2[Cl_3W(\mu\text{-Se})(\mu\text{-SePh})_2WCl_3]\cdot 2CH_2Cl_2$[28] and $[(Ph_2MeP)W(SePh)_2(\mu\text{-Se})]_2\cdot 2THF$[29] under mild conditions has been reported.

The dimeric structure of $\{[(Me_3Si)_2N]_2V(\mu\text{-Se})\}_2$ in the solid state was confirmed by X-ray diffraction. An ORTEP view of the molecule is shown in Figure 4, and selected bond lengths and bond angles are listed in Table 4. Each vanadium center is coordinated by two amido nitrogens and two bridging selenium atoms that link the distorted tetrahedra. As expected on the basis of steric repulsions, the Se−V−Se angles are the smallest about the metal centers (Se(1)−V(1)−Se(2) = 99.30(4)°; Se(1)−V(2)−Se(2) = 99.84(4)°), while the N−V−N

(25) Covalent radii of 1.16 and 1.36 Å for Se and Te, respectively, have been calculated from the E−Si bond lengths of a wide variety of complexes of $-ESi(SiMe_3)_3$.

(26) For examples of C−S bond cleavage in alkanethiolates, see: Boorman, P. M.; Fait, J. F.; Freeman, G. K. W. *Polyhedron* **1989**, *8*, 1762. Laurie, J. C. V.; Duncan, L.; Haltiwanger, R. C.; Weberg, R. T.; DuBois, M. R. *J. Am. Chem. Soc.* **1986**, *108*, 6234. Weberg, R. T.; Haltiwanger, R. C.; Laurie, J. C. V.; DuBois, M. R. *Ibid.* 6242. Dilworth, J. R.; Richards, R. L.; Dahlstrom, P.; Hutchinson, J.; Kumar, S.; Zubieta, J. *J. Chem. Soc., Dalton Trans.* **1983**, 1489. Kamata, M.; Yoshida, T.; Otsuka, S.; Hirotsu, K.; Higuchi, T. *J. Am. Chem. Soc.* **1981**, *103*, 3572. Boorman, P. M.; O'Dell, B. D. *J. Chem. Soc., Dalton Trans.* **1980**, 257. Examples of C−S bond cleavage in arene thiolates are more rare: Burrow, T. E.; Hughes, D. L.; Lough, A. L.; Maguire, M. J.; Morris, R. H.; Richards, R. L. *J. Chem. Soc., Dalton Trans.* **1995**, 2583. Listemann, M. L.; Schrock, R. R.; Dewan, J. C.; Kolodziej, R. M. *Inorg. Chem.* **1988**, *27*, 264. Adams, R. D.; Babin, J. E.; Kim. H. S. *J. Am. Chem. Soc.* **1987**, *109*, 1414.
(27) Batt, L. In *The Chemistry of Organic Selenium and Tellurium Compounds*; Patai, S., Rappoport, Z., Eds.; Wiley: New York, 1986; Vol. 1, p 157.
(28) Ball, J. M.; Boorman, P. M.; Fait, J. F.; Fraatz, H. B.; Richardson, J. F.; Collison, D.; Mabbs, F. E. *Inorg. Chem.* **1990**, *29*, 3290.
(29) Boorman, P. M.; Kraatz, H. B.; Parvez, M. *J. Chem. Soc., Dalton Trans.* **1992**, 3281.

Table 3. Comparison of Selected Metrical Parameters between $[(Me_3Si)_2N]_2VSeSi(SiMe_3)_3$, $[(Me_3Si)_2N]_2VTeSi(SiMe_3)_3$, and $[(Me_3Si)_2N]_2VTeSiPh_3$

$[(Me_3Si)_2N]_2VSeSi(SiMe_3)_3$		$[(Me_3Si)_2N]_2VTeSi(SiMe_3)_3$		$[(Me_3Si)_2N]_2VTeSiPh_3$	
		Bond Distances (Å)			
V−Se	2.451(1)	V−Te	2.6758(9)	V−Te	2.657(2)
$V-N_{av}$	1.926(4)	$V-N_{av}$	1.926(6)	$V-N_{av}$	1.92(1)
$N-Si_{av}$	1.729(6)	$N-Si_{av}$	1.727(8)	$N-Si_{av}$	1.73(2)
Se−Si	2.303(1)	Te−Si	2.527(1)	Te−Si	2.507(4)
V−C(1)	2.504(4)	V−C(1)	2.613(6)	V−C(1)	2.58(1)
V−C(7)	2.624(4)	V−C(7)	2.548(7)	V−C(7)	2.70(1)
V−H(1)	2.07(3)	V−H(1)	2.16(6)		
V−H(19)	2.17(3)	V−H(19)	2.04(7)		
		Bond Angles (deg)			
N(1)−V−N(2)	119.2(1)	N(1)−V−N(2)	120.4(2)	N(1)−V−N(2)	122.2(4)
N(1)−V−Se	119.84(9)	N(1)−V−Te	120.5(1)	N(1)−V−Te	113.7(3)
N(2)−V−Se	120.15(9)	N(2)−V−Te	118.5(1)	N(2)−V−Te	123.0(3)
V−N(1)−S(1)	100.0(1)	V−N(1)−S(1)	100.7(2)	V−N(1)−S(1)	100.3(5)
V−N(1)−Si(2)	133.8(2)	V−N(1)−Si(2)	135.6(2)	V−N(1)−Si(2)	131.1(6)
Si(1)−N(1)−Si(2)	125.4(2)	Si(1)−N(1)−Si(2)	122.7(2)	Si(1)−N(1)−Si(2)	128.3(6)
V−N(2)−Si(3)	100.4(1)	V−N(2)−Si(3)	100.4(2)	V−N(2)−Si(3)	104.7(6)
V−N(2)−Si(4)	136.3(2)	V−N(2)−Si(4)	131.4(2)	V−N(2)−Si(4)	129.1(5)
Si(3)−N(2)−Si(4)	122.8(2)	Si(3)−N(2)−Si(4)	128.1(2)	Si(3)−N(2)−Si(4)	125.7(6)
C(1)−V−C(7)	177.5(1)	C(1)−V−C(7)	175.9(2)	C(1)−V9C(7)	177.1(5)
V−Se−Si(5)	124.07(4)	V−Te−Si(5)	117.70(4)	V−Te−Si(5)	113.3(1)
Si(5)−Se−V−N(1)	117.6(1)	Si(5)−Te−V−N(1)	71.8(1)	Si(5)−Te−V−N(1)	120.0(3)
Si(5)−Se−V−N(2)	72.9(1)	Si(5)−Te−V−N(2)	116.6(1)	Si(5)−Te−V−N(2)	71.9(4)

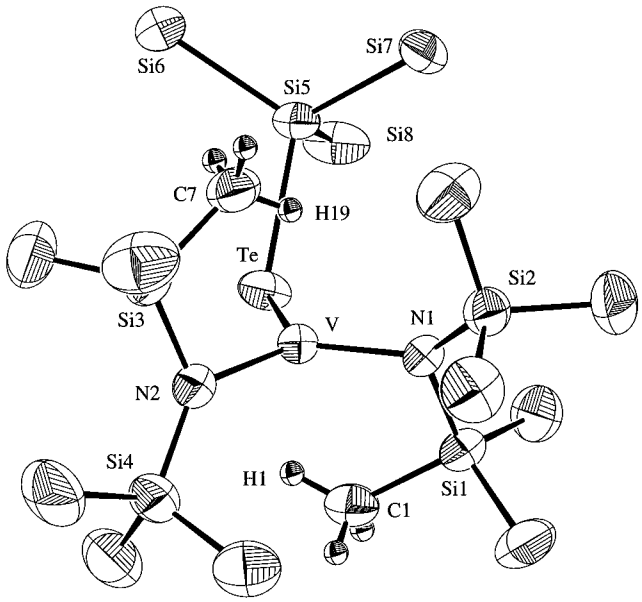

Figure 2. ORTEP drawing of $[(Me_3Si)_2N]_2VTeSi(SiMe_3)_3$. Thermal ellipsoids are drawn at 50% probability level. Methyl groups on −TeSi-$(SiMe_3)_3$ have been omitted for clarity.

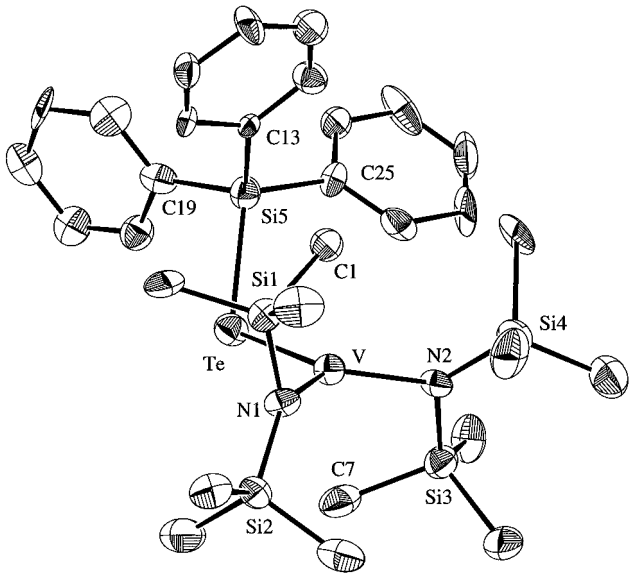

Figure 3. ORTEP drawing of $[(Me_3Si)_2N]_2VTeSiPh_3$. Thermal ellipsoids are drawn at 50% probability level.

angles are the largest (N(1)−V(1)−N(2) = 114.2(2)°; N(3)−V(2)−N(4) = 116.7(2)°). The V−N bond distances average 1.881(8) Å, slightly shorter than in the vanadium(III) compounds above, whereas the N−Si bond lengths are slightly elongated ($N-Si_{avg}$ = 1.77(1) Å). The four V−Se bonds average 2.364(2) Å and the V_2Se_2 core is folded in a slight butterfly conformation (Se(1)−V(1)−Se(2)−V(2) = 5.67(3)°); however the mean deviation from planarity within the ring is less than 0.06 Å. The Se(1)−Se(2) distance of 3.6106(7) Å is well outside the sum of the covalent radii (2.32 Å), ruling out the possibility of a μ-η^2-Se_2 ligand, and consistent with the proposed +4 oxidation state of the metals. Although the core is compressed roughly along the V(1)−V(2) vector such that the V−Se−V angles are about 80°, the V(1)−V(2) distance (3.044(1) Å) is indicative of a weak to nonexistent metal−metal bond. For comparison, the intermetallic distance in other vanadium(IV) dimers bridged by selenide ligands[30] range from 2.502(2) Å in (Cp*V)$_2$(μ-η^2-Se_2)(μ-Se)[31] to 2.779(5) Å in the polyselenide anion $[V_2Se_{13}][NEt_4]_2$.[32] The internuclear separation is somewhat longer in the square pyramidal compound $[V_2O_2Se_{10}][K]_4$ (2.90(1) and 2.96(1) Å for two independent molecules)[33] and the related $[V_2O_2Se_8][K]_4$ (2.958(7) Å).[33] Several of the peripheral methyl groups have C−Se distances that are significantly shorter than the sum of the van der Waals radii[34] (C(1)−Se(2) = 3.338(6) Å; C(7)−Se(1) = 3.325(6) Å; C(10)−Se(2) = 3.458(6) Å; C(16)−Se(2) = 3.292(6) Å; C(19)−Se(1) = 3.510(6) Å), a result that is perhaps not surprising considering the polarizability of selenium.

(30) Rheingold, A. L.; Bolinger, C. M.; Rauchfuss, T. B. *Acta Crystallogr.* **1986**,*C42*, 1878.
(31) Herberhold, M.; Kuhnlein, M.; Schrepfermann, M.; Ziegler, M. L.; Nuber, B. *J. Organomet. Chem.* **1990**, *398*, 259.
(32) Chau, C.-N.; Wardle, R. W. M.; Ibers, J. A. *Inorg. Chem.* **1987**, *26*, 2740.
(33) Liao, J.-H.; Hill, L.; Kanatzidis, M. G. *Inorg. Chem.* **1993**, *32*, 4650.
(34) The van der Waals radii of Se and -CH_3 are 1.87 and 2.12 Å, respectively. See Bondi, A. *J. Chem. Phys.* **1964**, *68*, 441.

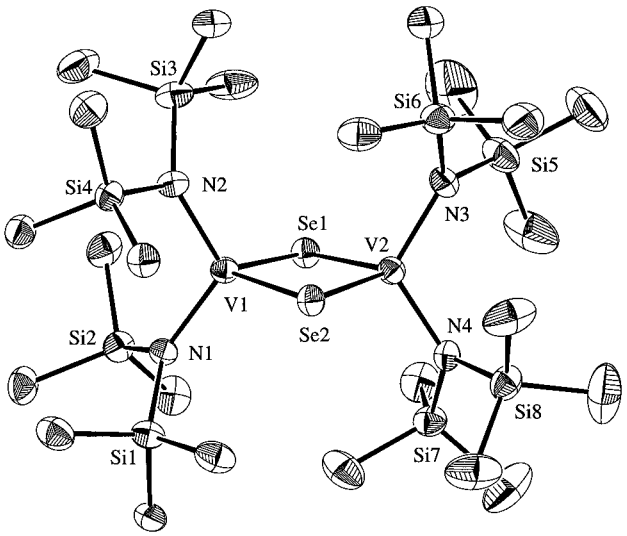

Figure 4. ORTEP drawing of $\{[(Me_3Si)_2N]_2V(\mu\text{-Se})\}_2$. Thermal ellipsoids are drawn at 35% probability level.

Table 4. Selected Metrical Parameters for $\{[(Me_3Si)_2N]_2V(\mu\text{-Se})\}_2$

Bond Distances (Å)			
V(1)−Se(1)	2.362(1)	V(1)−N(2)	1.888(4)
V(1)−Se(2)	2.375(1)	V(2)−N(3)	1.880(4)
V(2)−Se(1)	2.363(1)	V(2)−N(4)	1.868(4)
V(2)−Se(2)	2.356(1)	N−Si_{av}	1.77(1)
V(1)−N(1)	1.887(4)		

Bond Angles (deg)			
V(1)−Se(1)−V(2)	80.22(3)	N(2)−V(1)−Se(1)	114.1(1)
V(1)−Se(2)−V(2)	80.08(3)	N(2)−V(1)−Se(2)	109.0(1)
Se(1)−V(1)−Se(2)	99.30(4)	N(3)−V(2)−Se(1)	108.5(1)
Se(1)−V(2)−Se(2)	99.84(4)	N(3)−V(2)−Se(2)	114.5(1)
N(1)−V(1)−N(2)	114.2(2)	N(4)−V(2)−Se(1)	109.8(1)
N(3)−V(2)−N(4)	116.7(2)	N(4)−V(2)−Se(2)	106.2(1)
N(1)−V(1)−Se(1)	108.3(1)	Se(1)−V(1)−Se(2)−V(2)	5.67(3)
N(1)−V(1)−Se(2)	110.9(1)		

Scheme 1

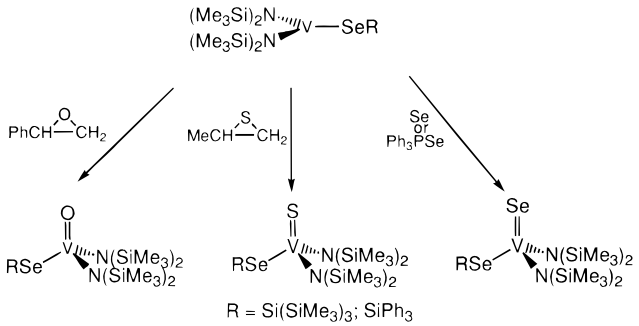

Vanadium(V) Chalcogenide−Chalcogenolates. As summarized in Scheme 1, $[(Me_3Si)_2N]_2V(SeR)$ (R = $Si(SiMe_3)_3$; $SiPh_3$) readily underwent $2e^-$ oxidation to the vanadium(V) chalcogenide complexes $[(Me_3Si)_2N]_2V(E)(SeR)$ (E = O, S, Se) on treatment with styrene oxide, propylene sulfide, and Ph_3PSe or gray selenium. As monitored by ^1H and ^{51}V NMR spectroscopy, the reactions were apparently very clean and immediate, except that with Se powder which proceeded slowly over 2 days. Attempts at preparing the selenolate−telluride species were unsuccessful as neither Te powder nor Et_3PTe reacted, even over prolonged periods. This is similar to what is observed with $[N_3N]V$ ($[N_3N] = [(Me_3SiNCH_2CH_2)_3N]$), where $[N_3N]V{=}Te$ was generated only by exposing a mixture of $[N_3N]V$ and $Me_3P{=}Te$ to a vacuum[35] and was susceptible to loss of Te^0.

The highly soluble $[(Me_3Si)_2N]_2V(E)[SeSi(SiMe_3)_3]$ (E = O, S, Se) derivatives were all isolated as deeply colored, crystalline solids from HMDSO in moderate yields (ca. 50%), and the selenide−selenolate has been structurally characterized (see below). The IR spectra possess the expected absorbances due to the $\nu_{V=O}$ (1012 cm^{-1}), $\nu_{V=S}$ (568 cm^{-1}), and $\nu_{V=Se}$ (455 cm^{-1}) moieties. For comparison, the $\nu_{V=E}$ stretching frequencies in $[EV(edt)_2]^{2-}$ (edt = 1,2-ethanedithiolate) are 930 (E = O), 502 (E = S), and 397 cm^{-1} (E = Se),[36] and those in a series of thio- and selenovanadium(IV) porphyrin complexes are 555−561 cm^{-1} (E = S) and 434−447 cm^{-1} (E = Se),[37] reflecting the weaker vanadium(IV)−chalcogenide bond. The $\nu_{V=O}$ compares best with those in the series of compounds $OV(Cl)_x(OR)_{3-x}$ (R = alkyl, x = 1, 2), which are generally in the range of 998−1019 cm^{-1}.[38−40] Along with the typical intraligand transition at about 220 nm (ϵ = 13 500−17 000 M^{-1} cm^{-1}), the UV−vis spectra contain a pair of charge-transfer bands that shift hypsochromically in the sulfide and selenide as compared to those in the oxo (nm (ϵ): E = O 512 (2 100), 364 (3 800); E = S 450 (2 900), 322 (7 800); E = Se 470 (2 000), 328 (5 500)). In contrast to what would be expected based on the electronegativity of the terminal chalcogenide, the resonances in the ^1H and $^{13}C\{^1H\}$ NMR spectra for the amido and selenolate trimethylsilyl substituents shift to progressively lower field as the terminal chalcogenide becomes heavier. The signals in the ^{51}V NMR spectra follow the same trend and show resonances at 245, 1102, and 1444 ppm for the oxo, sulfide, and selenide complexes respectively. The downfield shift of the central metal's NMR signal as the terminal chalcogenide ligand becomes less electronegative (or a weaker π-donor) is a well-established trend[31,35,41−46] and has been termed the inverse chalcogen effect. The line width of the ^{51}V NMR signals prevented the observance of a $J_{V,Se}$, and attempts at aquiring ^{77}Se NMR spectra were not successful, presumably due to the quadropolar ^{51}V nuclei (I = 7/2).

Chalcogen transfer reagents also reacted with $[(Me_3Si)_2N]_2$-$VTeSi(SiMe_3)_3$ (Scheme 2) and $[(Me_3Si)_2N]_2VTeSiPh_3$; however the vanadium(V) chalcogenide−tellurolates were less stable than the selenolates and susceptible to reduction. Treatment of $[(Me_3Si)_2N]_2VTeSi(SiMe_3)_3$ with 1 eq of styrene oxide resulted in a deep aqua solution from which $[(Me_3Si)_2N]_2V$-$(O)[TeSi(SiMe_3)_3]$ was isolated as dark blue crystals in 47% yield after workup in HMDSO. The compound is mildly sensitive to ambient light in solution (liberating $Te_2[Si(SiMe_3)_3]_2$) but does not appear to be photosensitive in the solid state. The IR spectrum of the oxo−tellurolate is identical to its selenolate counterpart in all respects ($\nu_{V=O}$ = 1012 cm^{-1}); however, the resonance at 504 ppm in its ^{51}V NMR spectrum is 259 ppm downfield of that for the selenolate. Its UV−vis

(35) Cummins, C. C.; Schrock, R. R.; Davis, W. M. *Inorg. Chem.* **1994**, *33*, 1448.
(36) Nicholson, J. R.; Huffman, J. C.; Ho, D. M.; Christou, G. *Inorg. Chem.* **1987**, *26*, 3030.
(37) Poncet, J. L.; Guilard, R.; Friant, P.; Goulon-Ginet, C.; Goulon, J. *Nouv. J. Chim.* **1984**, *8*, 583.
(38) Crans, D. C.; Chen, H.; Felty, R. A. *J. Am. Chem. Soc.* **1992**, *114*, 4543.
(39) Hillerns, F.; Rehder, D. *Chem. Ber.* **1991**, *124*, 2249.
(40) Witke, V. K.; Lachowicz, A.; Bruser, W.; Zeigan, D. *Z. Anorg. Allg. Chem.* **1980**, *465*, 193.
(41) Herberhold, M.; Schrepfermann, M.; Darkwa, J. *J. Organomet. Chem.* **1992**, *430*, 61.
(42) Herberhold, M.; Schrepfermann, M. *J. Organomet. Chem.* **1991**, *419*, 85.
(43) Feher, F. J.; Walzer, J. F. *Inorg. Chem.* **1991**, *30*, 1689.
(44) Devore, D. D.; Lichtenhan, J. D.; Takusagawa, F.; Maatta, E. A. *J. Am. Chem. Soc.* **1987**, *109*, 7408.
(45) Priebsch, W.; Rehder, D. *Inorg. Chem.* **1985**, *24*, 3058.
(46) Becker, K. D.; Berlage, U. *J. Magn. Reson.* **1983**, *54*, 272.

Scheme 2

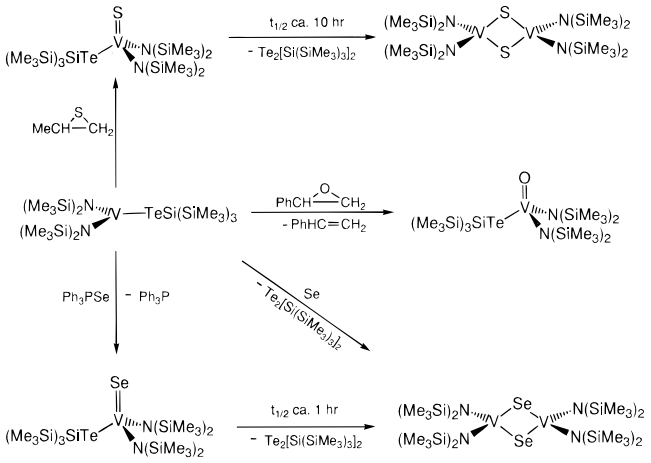

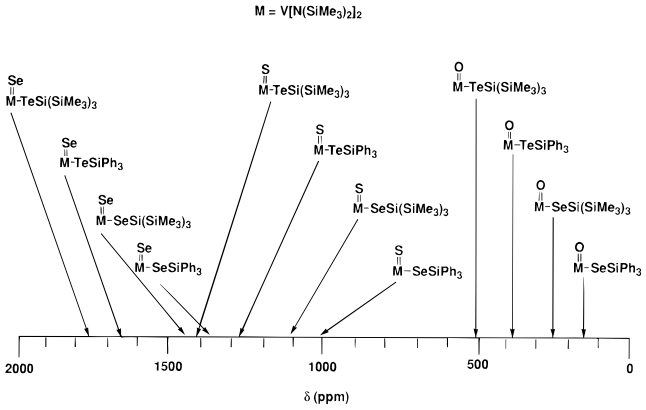

Figure 5. Graphical depiction of the ^{51}V NMR chemical shifts for vanadium(V) chalcogenide−chalcogenolates. Spectra were recorded in C_6D_6 at ambient temperature and chemical shifts (δ) are relative to $VOCl_3$ at 0 ppm.

spectrum is similar to the that of the $-SeSi(SiMe_3)_3$ complex, but the charge transer bands are slightly red shifted (nm (ϵ): 622 (2 100), 386 (4 100), 332 (5 300)). Photolysis of a C_6D_6 solution of the oxo−tellurolate rapidly yielded a forest green mixture that contained $Te_2[Si(SiMe_3)_3]_2$ as the only species detected in the ^{1}H and $^{13}C\{^1H\}$ NMR spectra; unfortunately no vanadium-containing compound could be isolated from preparative scale reactions. The photosensitivity of the oxo−tellurolate contrasts with the stability of the $-SeSi(SiMe_3)_3$ analog which was photolyzed for several hours without noticeable decomposition.

Propylene sulfide and Ph_3PSe each reacted with $[(Me_3Si)_2N]_2VTeSi(SiMe_3)_3$ to yield transient diamagnetic products that are presumably the sulfide− and selenide−tellurolates. These species were characterized by ^{1}H and ^{51}V NMR spectroscopy (Scheme 2). The dark (black) solution of the sulfide−tellurolate slowly decomposes ($t_{1/2}$ ca. 10 h) to afford maroon mixtures of $Te_2[Si(SiMe_3)_3]_2$ and a new product that gives a singlet in the ^{1}H NMR (δ 0.52). Although the latter product has not been fully characterized, at this point we tentatively formulate it as $\{[(Me_3Si)_2N]_2V(\mu\text{-S})\}_2$, the sulfide analog of $\{[(Me_3Si)_2N]_2V(\mu\text{-Se})\}_2$. Similarly, Ph_3PSe immediately transferred Se to $[(Me_3Si)_2N]_2VTeSi(SiMe_3)_3$ yielding $[(Me_3Si)_2N]_2V(Se)[TeSi(SiMe_3)_3]$ as the kinetic product. Most indicative of the selenide−tellurolate was its deshielded ^{51}V NMR resonance (δ 1755). The dark-colored mixture gradually turns emerald green over several hours, and monitoring the reaction by ^{1}H and ^{51}V NMR spectroscopy showed a smooth reaction to $Te_2[Si(SiMe_3)_3]_2$ and $\{[(Me_3Si)_2N]_2V(\mu\text{-Se})\}_2$ ($t_{1/2}$ ca. 3 h). The rate of the reaction qualitatively appears to be the same for samples that are stored in the dark, in contrast to the decomposition of the oxo−tellurolate whose rate of decompostion was photolytically accelerated. The bis(μ-Se) dimer may be obtained directly by the reaction of $[(Me_3Si)_2N]_2VTeSi(SiMe_3)_3$ with Se for 2 days in hexanes (80−90%); however the product is not as pure as that obtained from the reaction between $[(Me_3Si)_2N]_2V(Br)(THF)$ and (DME)LiSeC($SiMe_3$).

Diamagnetic derivatives that we formulate as $[(Me_3Si)_2N]_2V(E)(TeSiPh_3)$ (E = O, S, Se) were similarly generated in solution and characterized by ^{1}H and ^{51}V NMR spectroscopy. The ink-purple $[(Me_3Si)_2N]_2V(O)(TeSiPh_3)$ and the brown sulfide and selenide complexes were in all cases less stable than even the $[(Me_3Si)_2N]_2V(E)(TeSi(SiMe_3)_3)$ complexes. For example, $[(Me_3Si)_2N]_2V(S)(TeSiPh_3)$ decomposed ($t_{1/2}$ ca. 8 h) to give a mixture of products that contained $\{[(Me_3Si)_2N]_2V(\mu\text{-S})\}_2$ as the primary vanadium-containing species detected by ^{1}H NMR spectroscopy. The selenide analog, $[(Me_3Si)_2N]_2V(Se)(TeSiPh_3)$, was even more unstable, decomposing cleanly to $\{[(Me_3Si)_2N]_2V(\mu\text{-Se})\}_2$ ($t_{1/2}$ ca. 15 min).

The ^{51}V NMR chemical shifts for all of the chalcogenide−chalcogenolate are depicted graphically in Figure 5. Along with the general downfield progression as the terminal chalcogenide becomes heavier, two additional trends emerge. First, within a particular group of $[V{=}E]^{3+}$ compounds, the selenolate derivatives all have ^{51}V signals upfield of those in the tellurolates. Since, for example, the vanadium−oxo stretching frequency was the same in $[(Me_3Si)_2N]_2V(O)[ESi(SiMe_3)_3]$ (E = Se, Te) ($\nu_{V=O}$ = 1012 cm^{-1}), it seems reasonable to attribute the observed differences in chemical shifts to any coordinative differences between the −ER ligands. While simple inductive effects may operate in a way opposite to what may be expected (e.g., the "inverse chalcogen effect"), it has been demonstated that the replacement of simple σ-donor ligands with ligands that are better π-donors is coincident with and upfield shift in the ^{51}V NMR signals.[43] Thus, it may be that the selenolates act as marginally better π-bases than do the tellurolates in this system, as would be expected based on the lower energy 4p orbitals of Se.[47] Secondly, the -$SiPh_3$ derivatives show ^{51}V NMR signals that are consistently upfield from the $-Si(SiMe_3)_3$ substituted chalcogenolates. Again it would appear that an electronic difference between the silyl groups should account for this trend, although the magnitude of the shifts are relatively small (ca. 100 ppm) considering the large chemical shift range of ^{51}V. In light of the limited data in hand, the most significant aspect of the trend is its persistency.

Styrene oxide readily transfers oxygen to $[(Me_3Si)_2N]_2V(Br)(THF)$ yielding the diamagnetic oxo-derivative in about 70% yield (eq 3). In contrast, propylene sulfide or Ph_3PSe did not

$$[(Me_3Si)_2N]_2V(Br)(THF) \xrightarrow[-PhCH{=}CH_2,\ -THF]{PhCH(O)CH_2} [(Me_3Si)_2N]_2V(O)(Br) \quad (3)$$

cleanly react to yield the sulfide or selenide compounds under similar conditions. The oxo−bromide was isolated as orange crystals in 70% yield after crystallization from HMDSO. It is characterized by a strong absorbance at 1004 cm^{-1} ($\nu_{V=O}$) in the IR spectrum and singlets in the ^{1}H,$^{13}C\{^1H\}$, and ^{51}V NMR spectra. The latter resonance comes at δ −18 ppm, well upfield from the oxo−chalcogenolates.

(47) Since alkoxides are considered much better π donors than thiolates, a more dramatic demonstration of this effect is seen between the ^{51}V NMR shifts in $OV(OSiPh_3)_3$ (δ −725) and $OV(SSiPh_3)_3$ (δ 592). See: Preuss, F.; Noichl, H. *Z. Naturforsch.* **1987**, *B42*, 121.

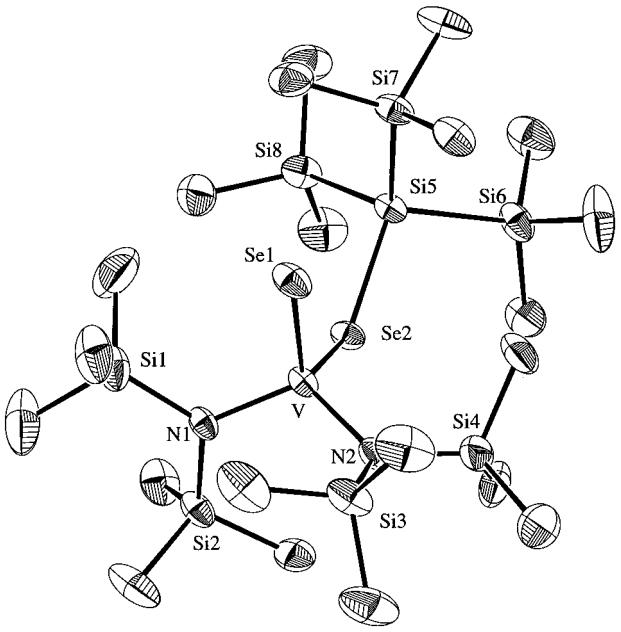

Figure 6. ORTEP drawing of $[(Me_3Si)_2N]_2V(Se)[SeSi(SiMe_3)_3]$. Thermal ellipsoids are drawn at the 35% probability level. Methyl groups on $-SeSi(SiMe_3)_3$ have been omitted for clarity.

Table 5. Selected Metrical Data for $[(Me_3Si)_2N]_2V(Se)[SeSi(SiMe_3)_3]$

Bond Distances (Å)			
V−Se(1)	2.1754(9)	V−N(2)	1.881(4)
V−Se(2)	2.3620(8)	Se(2)−Si(5)	2.326(1)
V−N(1)	1.860(4)	N−Si_{av}	1.774(8)
Bond Angles (deg)			
Se(1)−V−N(1)	109.0(1)	Se(1)−V−Se(2)−Si(5)	8.13(7)
Se(1)−V−N(2)	108.0(1)	V−Se(2)−Si(5)−Si(7)	0.8(1)
Se(1)−V−Se(2)	108.26(3)	Se(1)−V−N(1)−Si(1)	17.3(3)
Se(2)−V−N(1)	104.9(1)	Se(1)−V−N(1)−Si(2)	177.8(2)
Se(2)−V−N(2)	111.6(1)	Se(1)−V−N(2)−Si(3)	63.3(2)
N(1)−V−N(2)	114.8(2)	Se(1)−V−N(2)−Si(4)	95.9(2)
V−Se(2)−Si(5)	127.42(4)		

The X-ray structure of $[(Me_3Si)_2N]_2V(Se)[SeSi(SiMe_3)_3]$ affords a unique opportunity to compare the bond lengths of singly and doubly bonded selenium to a single metal center. An ORTEP view of the molecule is shown Figure 6, and selected metrical data is collected in Table 5. The angles about the vanadium range from a minimum of 104.9(1)° (Se(2)−V−N(1)) to a maximum of 114.8(2)° (N(1)−V−N(2)). The V−N and N−Si bond lengths are similar to those in the dimeric vanadium(IV) structure discussed above ($V-N_{avg} = 1.871(6)$ Å; $N-Si_{avg} = 1.774(8)$ Å). The bulky $-Si(SiMe_3)_3$ substituent of the selenolate is displaced slightly toward the N(2) amido group (Se(1)−V−Se(2)−Si5 = 8.13(7)°) and oriented such that the V−Se(2) and Si(5)−Si(7) bonds are nearly eclipsed (V−Se(2)−Si(5)−Si(7) = 0.8(1)°). This allows two methyl groups (C(16) and C(18)) to flank either side of the terminal selenide ligand. The V−Se(2) single bond length (2.3620(8) Å) is identical to those observed in the bis(μ-Se) dimer, while the V−Se(1) double bond length (2.1754(9) Å) is contracted by about 8%. In the dianion $[VSe(edt)_2]^{2-}$,[36] the only other structurally characterized V−Se multiple bond, the V−Se distance is 2.196(3) Å. The slightly longer bond distance in the latter is expected due the lower oxidation state of the metal center and is consistent with its lower energy $\nu_{V=Se}$ in the IR spectrum (397 versus 455 cm^{-1}).

Oxo−Amido to Siloxide−Imido Isomerization. The synthetic utility of silyl group migrations has been exploited for many years.[48] A general synthesis of transition metal imido complexes[49] is the reaction between metal oxo−chlorides and trimethylsilyl amines, as illustrated generally in eq 4. These

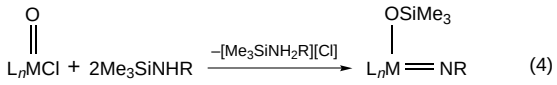

(4)

reactions apparently proceed through intermediate oxo−silylamides, which then rearrange to the observed products. In the same way, reactions between $OMCl_3$ (M = V,[50] Nb,[51] Ta[51]) and 3 equiv of lithium or sodium bis(trimethylsilyl)amide yield $[(Me_3Si)_2N]_2(Me_3SiN)M(OSiMe_3)$ as the isolated products. Examples in group 6 include the reaction between CrO_2Cl_2 and $HN(Bu^t)(SiMe_3)$ to yield $Cr(NBu^t)_2(OSiMe_3)_2$[52] however the related reaction with $HN(SiMe_3)_2$ affords $CrO_2[N(SiMe_3)_2]_2$;[52] MO_2Cl_2 (M = Mo, W) gives only imido−siloxide products in similar reactions.[52] It seems clear that, in most systems, the free energy of the siloxide−imido is usually lower than that of the isomeric oxo−silylamido; thus, assuming it is kinetically accessible, rearrangement to the former will occur. It is noteworthy that molecules of the type $[(Me_3Si)_2N]_3MO$ (M = Nb,[53] Re,[54] U[55]) have been isolated.

As noted above, $[(Me_3Si)_2N]_2V(O)[SeSi(SiMe_3)_3]$ was photolyzed for extended periods without any sign of decompostion. However, on heating toluene solutions of the complex at reflux (16 h), the rearranged imido−siloxide was isolated in about 50% yield (eq 5). Reactions monitored by NMR spectroscopy in the

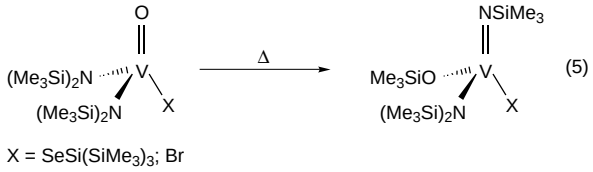

(5)

presence of an internal standard (C_6Me_6) showed a 70% conversion to product, with $HN(SiMe_3)_2$ as the only other detected species. Presumably a paramagnetic vanadium byproduct(s) is also formed through a competitive reaction. The siloxide−imido product is well characterized by its ^1H and $^{13}C\{^1H\}$ NMR spectra, which show the expected 2:1:1 ratio of signals. Most prominent of the differences between the IR spectra of the isomers is the replacement of the $\nu_{V=O}$ (1012 cm^{-1}) in the spectrum of the starting material with the $\nu_{as(V=N-Si)}$ (1095 cm^{-1}) and $\nu_{as(V-O-Si)}$ (927 cm^{-1}) in that of the product. These last two bands are of somewhat lower energy than those observed for the product when $X = -N(SiMe_3)_2$,[51] synthesized by the reaction of $OVCl_3$ with 3 equiv of $NaN(SiMe_3)_2$. Both isomers are volatile under the conditions of EI-MS, showing a strong peak for the molecular ion. It is interesting that the ^{51}V NMR signal for the product (δ 8.7) is 236 ppm upfield of that for the starting material (δ 245), indicating that an increase of

(48) Brook, A. G.; Bassindale, A. R. In *Rearrangements in Ground and Excited States*; de Mayo, P., Ed.; Academic Press: New York, 1980; Vol. 2; p 149.
(49) Wigley, D. E. In *Progress in Inorganic Chemistry*; Karlin, K. D., Ed.; Wiley: New York, 1994; Vol. 42, p 239.
(50) Burger, H.; Smrekar, O.; Wannagat, U. *Monatsh. Chem.* **1964**, *95*, 292.
(51) Herrmann, W. A.; Denk, M.; Dyckhoff, F.; Behm, J. *Chem. Ber.* **1991**, *124*, 2401.
(52) Lam, H.-W.; Wilkinson, G.; Hussain-Bates, B.; Hursthouse, M. B. *J. Chem. Soc., Dalton Trans.* **1993**, 1477.
(53) Hubert-Pfalzgraf, L. G.; Tsunoda, M. *J. Chem. Soc., Dalton Trans.* **1988**, 533.
(54) Edwards, P. G.; Wilkinson, G.; Hursthouse, M. B.; Malik, K. M. A. *J. Chem. Soc., Dalton Trans.* **1980**, 2467.
(55) Andersen, R. A. *Inorg. Chem.* **1979**, *18*, 1507.

electron density at vanadium may also be important (along with Si−O bond formation) as a driving force in the reaction. As mentioned above, if X = $TeSi(SiMe_3)_3$, reduction of the vanadium is presumably a lower energy reaction pathway since oxidized ligand (i.e., $Te_2[Si(SiMe_3)_3]_2$) was the only species detected after the compound's thermal or photolytic decomposition.

The analogous isomerization of $[(Me_3Si)_2N]_2V(O)(Br)$ was much more facile (e.g., $t_{1/2}$ = 11.8 min in C_6D_6 at 85 °C) than for the selenolate derivative and proceeded quantitatively to the siloxide−imido. Spectroscopically, the differences between the product and starting material are analogous to those noted above. Kinetic data for the reaction in C_6D_6 was collected in the temperature range 62−95 °C.[56] The disappearance of starting material and the appearance of product were monitored by ^1H NMR spectroscopy. The data are consistent with a first-order reaction and thus implicate an intramolecular isomerization. The activation parameters ($\Delta H^{\ddagger} = 26 \pm 1$ kcal mol^{-1} and $\Delta S^{\ddagger} = -0.60 \pm 2$ eu) are comparable to those measured for the first-order, thermal rearrangement of β-ketosilanes to siloxyalkenes,[57,58] and in fact in some of these latter systems, the two isomers are in tautomeric equilibrium.[48] Whether these reactions proceed via a concerted transition state or a five-coordinate silicon intermediate has been debated.[59] Nonetheless, it is clear that the rearrangements are mediated through hypervalent silicon. The sulfide- and selenide−selenolate also decomposed when heated to 110 °C, but in these cases the reactions were not as clean as with the oxo derivatives.

Acknowledgment. We are grateful to the National Science Foundation for financial support and the Alfred P. Sloan Foundation for the award of a research fellowship to J.A.

Supporting Information Available: ORTEP drawings with complete atomic numbering and complete listings of bond distances and angles and positional and thermal parameters for $[(Me_3Si)_2N]_2VSeSi(SiMe_3)_3$, $[(Me_3Si)_2N]_2VTeSi(SiMe_3)_3$, $[(Me_3Si)_2N]_2VTeSiPh_3$, $\{[(Me_3Si)_2N]_2V(\mu\text{-}Se)_2\}_2$, and $[(Me_3Si)_2N]_2V(Se)[SeSi(SiMe_3)_3]$ (30 pages). Ordering information is given on any current masthead page.

IC960439L

(56) The experimentally determined rate constants ($k_{exp} \times 10^4$) were as follows: $k_{62°} = 0.686$ s^{-1}; $k_{75°} = 3.55$ s^{-1}; $k_{80°} = 5.30$ s^{-1}; $k_{85°} = 9.79$ s^{-1}; $k_{90°} = 15.2$ s^{-1}; $k_{95°} = 25.1$ s^{-1}.

(57) Brook, A. G.; MacRae, D. M.; Bassindale, A. R. *J. Organomet. Chem.* **1975**, *86*, 185.
(58) Larson, G. L.; Fernandez, Y. V. *J. Organomet. Chem.* **1975**, *86*, 193.
(59) Kwart, H.; Barnette, W. E. *J. Am. Chem. Soc.* **1977**, *99*, 614.